Exploring a Novel Public-Private-Partnership Data Sharing Policy through a collaborative Arterial Traffic Management System (CTEDD 021-02)

Swastik Khadka, graduate student (UTA)
Pengfei (Taylor) Li*, Ph.D., P.Eng.(UTA, PI)
Somdut Roy, graduate student (GaTech)
Michael Hunter, Ph.D. (GaTech, Co-PI)
Angshuman Guin Ph.D. (GaTech)

FINAL REPORT

CTEDD
Center for Transportation Equity, Decisions & Dollars

Exploring a Novel Public-Private-Partnership Data Sharing Policy through a collaborative Arterial Traffic Management System

By:

Swastik Khadka
Graduate Research Assistant
Department of Civil Engineering
The University of Texas at Arlington, Arlington, TX, 76019 USA
Email: swastik.khadka@mavs.uta.edu

Pengfei (Taylor) Li, Ph.D., P.Eng.
Assistant Professor
Department of Civil Engineering,
The University of Texas at Arlington, Arlington, TX, 76019 USA
Email: Taylor.Li@uta.edu ; Tel: 817-272-3416

Somdut Roy
School of Civil and Environmental Engineering
Georgia Institute of Technology
788 Atlantic Drive NW
Atlanta, GA 30332, USA Tel: 678-602-3220
somdut.roy@gatech.edu

Michael Hunter, Ph.D.
School of Civil and Environmental Engineering
Georgia Institute of Technology
788 Atlantic Drive NW
Atlanta, GA 30332, USA
Tel: 404-385-1243
michael.hunter@ce.gatech.edu

Angshuman Guin, Ph.D.
School of Civil and Environmental Engineering
Georgia Institute of Technology
788 Atlantic Drive NW
Atlanta, GA 30332, USA Tel: 404-894-5830
angshuman.guin@gatech.edu

Sponsorship:
CTEDD

For:
Center for Transportation, Equity, Decisions and Dollars **(CTEDD)**
USDOT University Transportation Center
The University of Texas at Arlington
Woolf Hall, Suite 325
Arlington TX 76019 United States
Phone: 817-272-5138 | Email: c-tedd@uta.edu

In cooperation with United States Department of Transportation's Office of Research, Development, and Technology (RD&T)

Acknowledgments

This research is partially supported by the project "Exploring a Novel Public-Private-Partnership Data Sharing Policy through a collaborative Arterial Traffic Management System" sponsored by the USDOT UTC Center, Center for Transportation Equity, Decisions, and Dollars (CTEDD). The ICV data are distributed by Wejo Data Service Inc. The traffic signal log data were retrieved from the traffic operations centers in Cities of Arlington, Frisco and Fort Worth.

Disclaimer

The contents of this report reflect the views of the authors, who are responsible for the facts and the accuracy of the information presented herein. This document is disseminated under the sponsorship of the U.S. Department of Transportation's University Transportation Centers Program, in the interest of information exchange. The Center for Transportation, Equity, Decisions and Dollars (CTEDD), the U.S. Government and matching sponsor assume no liability for the contents or use thereof.

Technical Report Documentation Page

1. Report No.	2. Government Accession No.	3. Recipient's Catalog No.
CTEDD 020-02		

4. Title and Subtitle

Exploring a Novel Public-Private-Partnership Data Sharing Policy through a collaborative Arterial Traffic Management System

5. Report Date

04 April 2023

6. Performing Organization Code

7. Author(s)

Part I:
Swastik Khadka, graduate student (UTA), orchid 0000-0002-5323-3081
Pengfei (Taylor) Li*, Ph.D., P.Eng.(UTA, PI), orchid 0000-0002-3833-5354

Part II:
Somdut Roy, graduate student (GaTech)
Michael Hunter, Ph.D. (GaTech, Co-PI)
Angshuman Guin Ph.D. (GaTech)

8. Performing Organization Report No.

9. Performing Organization Name and Address

The University of Texas at Arlington
Department of Civil Engineering
Box 19308
The University of Texas at Arlington
Arlington, TX
76019-0308

Georgia Institute of Technology
School of Civil and Environmental Engineering
788 Atlantic Drive NW
Georgia Institute of Technology
Atlanta, GA
30332, USA

10. Work Unit No. (TRAIS)

11. Contract or Grant No.

12. Sponsoring Organization Name and Address

Center for Transportation, Equity, Decisions and Dollars (CTEDD)
USDOT University Transportation Center

13. Type of Report and Period Covered

Final Report

14. Sponsoring Agency Code

The University of Texas at Arlington
Woolf Hall, Suite 325
Arlington TX 76019 United States

15. Supplementary Notes

Additional project information is available at CTEDD 020-02 (https://ctedd.uta.edu/research-projects/embracing-emerging-internet-based-traffic-big-data-in-smart-city-applications-to-improve-transportation-systems-efficiency-safety-and-equity%EF%BF%BC/). Project performed under a grant from the U.S. Department of Transportation's University Transportation Centers (UTC) Program.

16. Abstract

Part I

Connected vehicle (CV) data in this paper refer to the in-vehicle telematic data, including trajectories and driving events (e.g., hard braking) collected by vehicle manufacturers when vehicles are moving. Recently manufactured vehicles are equipped with cellular modems and Internet-of-Things (IoT) devices to collect vehicle data. Such data, after removing personal information, are being redistributed to 3rd-party organizations. Compared to other probe vehicle data, the CV data has a higher penetration rate, ubiquitous coverage, and almost lane-level positioning accuracy. These features pave the road for novel transportation applications in transportation planning and traffic operations. In this paper, we represent a novel framework to estimate the regional link volumes based on the CV data and a deep neural network (DNN) model. The training data are generated according to the link volumes (targeted model output) and the corresponding CV counts (input features) at the same locations. The DNN model's performance was compared with other estimation methods like linear regression and random forest and showed superior performance. The trained DNN model takes ubiquitous CV counts from other locations to estimate the corresponding link volumes. As a case study, the proposed DNN model was trained with a large training data set derived from CV data and time-dependent link counts collected at over 1,200 locations on the freeways in the Dallas-Fort-Worth area. The results reveal good accuracy and robustness.

17. Key Words	**18. Distribution Statement**
Crowdsourced data, connected vehicle, congestion management, transportation planning, transportation management	No restrictions. This document is available to the public through the Transport Research International Documentation (TRID) repository.

19. Security Classification (of this report)	**20. Security Classification (of this page)**	**21. No. of Pages**	**22. Price**
Unclassified.	Unclassified.	77	N/A

Summary

In Part I of this report, we present our efforts in exploring a new type of traffic data, referred to as internet-connected vehicle or ICV data for traffic congestion management and operational planning. Most currently manufactured vehicles contain on-board GPS and cellular modules, and they constantly connect to automobile manufacturers' clouds via cellular networks and upload their status. Some automobile manufacturers have recently redistributed the non-personal part of such data, such as geolocation, to the 3rd party for innovative applications. Compared with the traditional vehicle GPS data, the ICV data contain high-resolution GPS waypoints accompanied with the vehicles' abnormal moving events (e.g., hard braking). The ICV data also has huge potential in congestion management and operational planning. We explore to identify and analyze congestions on both freeways and arterials using the ICV data. The ICV data adopted for this research are redistributed by Wejo Data Service Inc., representing 10% to 15% of all moving vehicles in the Dallas-Fort-Worth (DFW) area in Texas. Through one case study for a freeway segment and one for an arterial segment, we present new traffic performance metrics based on the characteristics of ICV data. The highlights of these efforts include (I) queue length and propagation at freeway bottlenecks can be directly measured based on where and when most internet-connected vehicles slow down and join the queue; (II) an internet-connected vehicle's actual delay time on arterials can be directly measured according to its slow movement percentage, without assuming the non-delay travel speed; (III) the ICV data set are also combined with the high-resolution traffic signal events to generate a "ground-truth" time-space diagram (TSD) on arterials,

a common visualization of arterial signal performance for transportation planning and operations.

In Part II, we explore the data generated by emergency vehicles and the impact on traffic operations. Emergency Vehicles (EVs), such as firetrucks, ambulances, etc. operate with the purpose of saving lives and mitigating property damage. Even small delays in their arrival could lead to catastrophic consequences. Emergency vehicle preemption (EVP) is implemented to provide the right-of-way to EVs by displaying the green indications solely along the EV route to the incident location. This paper evaluates the effectiveness of different preempt control strategies over a series of signalized intersections on an arterial in Norcross, Georgia. The study proposes a strategy, terming it “Dynamic Preemption”, which utilizes Connected Vehicle (CV) technology to detect the need for preemption prior to the EV reaching the vicinity of the intersection, utilizing real-time data streams.

The best EVP strategy maximizes the improvement in EV route while minimizing the adverse effect of preemption on the traffic in conflicting directions. Therefore, the effectiveness of EVP is measured for: (a) the EV route, which is chosen to be along the mainline for this case study, and (b) the side streets, which are expected to be adversely affected by preemption. The study tests different preemption strategies under varying scenarios over multiple replicates runs and provides a methodology for selecting the most favorable control strategy. It was seen that the potential exists, for the given corridor and scenario, for EV travel time improvements on the order of 25% with minimal impact to the conflicting traffic.

Key words: Crowdsourced data, connected vehicle, congestion management, Traffic Signals, Emergency Vehicle Preemption, preemption, dynamic preemption

Table of Contents

Part I

Table of Contents

Part II

List of Figures
Part I

List of Figures
Part II

Part I

Developing Novel Performance Measures for Traffic Congestion Management and Operation Planning Based on Connected Vehicle Data

Swastik Khadka

Graduate Research Assistant

Department of Civil Engineering

The University of Texas at Arlington, Arlington, TX, 76019 USA

Email: swastik.khadka@mavs.uta.edu

Pengfei (Taylor) Li, Ph.D., P.Eng.

Assistant Professor

Department of Civil Engineering,

The University of Texas at Arlington, Arlington, TX, 76019 USA

Email: Taylor.Li@uta.edu ; Tel: 817-272-3416

1. Introduction

The era of mobile computing enables ubiquitous smartphones, in-vehicle internet-of-things (IOT) devices as well as connected and automated vehicles. Vehicles and infrastructure are connected in multiple ways. One approach is through crowdsourcing. The mobile devices are generating rich traffic data sets of new types, which will be supplemental to the infrastructure sensors maintained by public agencies to better plan the traffic congestion management heavily driven by data. Collecting and maintaining infrastructure sensors at large scale requires a huge amount of construction and recurrent operational costs. Furthermore, infrastructure sensors are fixed-spot and therefore they cannot provide a full-spectrum of traffic conditions. Most agencies today still use the traffic data collected via fixed-spot infrastructure data for performance monitoring, such as inductive loops, road-side cameras and radar sensors (Xu et al. 2016). Some agencies also adopt automated vehicle identification techniques, such as Toll Tag ID (Turner et al. 2000) and Wi-Fi/Bluetooth MAC address matching(Li and Souleyrette 2016; Namaki Araghi et al. 2016). While these techniques are proven effective, bias are inevitable because the agencies have to empirically select sensors' locations and use point-to-point vehicle ID matching mechanism to represent the entire highway segments. In reality, congestions and bottlenecks may occur at any place and they contribute to a major portion of congestions on highways. Infrastructure detectors can only report the traffic conditions at certain fixed spots. As a result, the corresponding traffic performance monitoring is inevitably biased. One straightforward solution is to deploy infrastructure sensors more intensively to narrow the link segments while this option may be not cost-effective to agencies. On arterials, while intersections are explicit bottlenecks, hidden bottlenecks often exist at mid-block drive ways or two-way left-turn lanes. Such hidden

bottlenecks can hardly be identified with traditional traffic analytics or fixed-spot detector data.

To overcome these challenges and to provide new cost-effective solutions, we exploit the potential of emerging internet-connected vehicle (ICV) data in congestion management. The ICV data are passively crowdsourced and collected by automobile manufacturers. Most currently manufactured vehicles constantly connect to automobile manufacturer's clouds and upload their real-time status (e.g., the GMC's "OnStar", an add-on service based on subscriptions). Some automobile manufacturers have recently decided to redistribute such data sets (after removing the private info) to the 3rd party for innovative mobility applications. Compared with the traditional vehicle GPS data set, the ICV data contain high-fidelity waypoint locations accompanied with abnormal events (e.g., hard braking) while vehicles are moving. After some preliminary experiments, we conclude that the ICV data are highly accurate and hold great promises in congestion management. The ICV data are based on vehicle trips. Each trip will be allocated with a unique ID. For each waypoint of a trip, vehicle's instantaneous latitude, longitude, current timestamp, speed and heading are provided. Abnormal vehicle maneuvers (e.g., hard braking) are also collected from on-board units. The ICV data for this study are procured from Wejo Data Service which is licensed by the General Motors. The penetration of the ICV data we studied represent 10%~15% of all moving vehicles in the Dallas-Fort-Worth (DFW) area, Texas, US.

The paper is organized as follows. Literature on traffic data collection and applications is reviewed first; then a scalable framework of processing the ICV data is presented. Third, two case studies are conducted to find the hidden highway bottlenecks, accompanied

with new performance metrics based on the ICV data sets; Third, we present new traffic performance metrics on arterials based on the ICV data and high-resolution traffic control log data.

2. Literature review

Congestion management on highways focus on bottleneck identification and mitigation. Traditional methods to discover bottlenecks mostly are based on infrastructure sensors. With fixed-spot detectors, Chen et al. design a statistical method to identify the possible appearance of bottlenecks on freeways by comparing the speed differences between the upstream and downstream locations. If the speed difference is more than 20 miles per hour, then a bottleneck is identified (Chen et al. 2004). Other than the speed reduction between locations, bottlenecks on freeways can also be identified by the duration of speed reduction at certain locations (Banks 2009), by the reduction of traffic volumes (Bertini 2003), by occupancy changes (Hall and Agyemang-Duah 1991; Zhang and Levinson 2004). The advantage of the fixed-spot detectors is that they can almost capture 100% of vehicle presence (if lane-by-lane detection is configured) and therefore reported results are accurate. However, selection of sensor locations is very important and hidden bottlenecks may be difficult to find.

Transportation agencies also explore to capture and match a small portion of vehicle “signatures” to collect segment travel time samples. The vehicle “signatures” refer to unique in-vehicle IDs. Through various road-side sniffing devices deployed at different locations, those unique vehicle IDs can be captured and re-matched. The time difference between road-side devices is considered a segment (i.e., space) travel time sample. Available vehicle signatures include but are not limited to: probe vehicle with known IDs

(Hofleitner et al. 2012), toll tags series numbers (Turner et al. 2000), license plate numbers (Bertini et al. 2005; Xu et al. 2011), cellphone locations (Qiu et al. 2009), vehicle's optical image identification (Kuroiwa et al. 2007), vehicles' magnetic signature matching (Charbonnier et al. 2012; Kavaler et al. 2011; Kwong et al. 2009; Sanchez et al. 2011; Sanchez et al. 2011) and Bluetooth MAC address matching(Bakula et al. 2012; Barcelo et al. 2010; Brennan et al. 2010; Haghani et al. 2010; Hainen et al. 2011; Quayle et al. 2010; Richardson et al. 2011). Segment travel time is a direct indictor of road congestion and considered superior to the estimated travel time by the fixed-spot detectors. Nonetheless, there are also challenges in leveraging between screening the sample outliers and sample sizes. For instance, the commonly used Bluetooth-based travel time estimation method, the sample size is usually less than 5%. To increase the capturing rate, high-gain antennas (with the sensing radius of 1,000 or more feet) must be used, resulting in large measure errors. In the meanwhile, vehicles are not tracked between two locations and their abnormal behaviors (e.g., pullover) cannot be tracked. As a result, the sample outliers must be screened. Other techniques also have their own drawbacks. Many research efforts have been dedicated to address these issues. As examples, A framework including multiple heuristic steps to process the Bluetooth-based travel time samples were designed by Hagahni et al. (Haghani et al. 2010) In their framework, a set of 24-hour historical travel time samples are selected to infer the travel speed's distributions. A moving standard deviation is designed by Quayle et al. to screen the Bluetooth-based travel time outlier samples (Quayle et al. 2010). Li and Souleyrette propose a Kalman-filter framework to estimate the time-varying travel time with collected Bluetooth travel time samples (Li and Souleyrette 2016). In category, these techniques

fall into the category of “passive sensing” technique. Road-side capturing devices are typically needed at different locations for travel time estimations.

After entering the era of mobile computing, most vehicles become "probe vehicles" via drivers’ smartphone apps and on-board units. These vehicles share their information regularly. The information can be collected through drivers’ smartphones, in-vehicle global positioning system (GPS) receivers, etc. Most new vehicles today are equipped with in-vehicle GPS receivers for location services (e.g., GM’s OnStar service). Such services require vehicles constantly share their locations and therefore the collected location data are essentially crowdsourced, and the non-personal part of such data sets is a novel traffic data set with massive sample sizes and broad coverages. The commercial probe vehicle data are typically provided in two forms: (I) dynamic link travel times/ link travel speeds according to aggregated GPS trajectories; (II) individual vehicle trips containing all the trip waypoints at small time intervals (3 s~15 s). Both types of GPS probe data are currently used in congestion management. For example, Gong and Fan design a framework to identify freeway bottlenecks using the large-scale link travel time aggregated from vehicle GPS trajectories (Gong and Fan 2018). They combine both probe data sets and traffic management center data to identify bottlenecks. Zhao et al. use commercial vehicle GPS trajectories with a time interval of 15 s or longer to evaluate traffic progression in Washington (Zhao et al. 2013). Waddell et al. investigate to estimate traffic signal performance along arterials using the vehicle GPS trajectories and automated traffic signal performance metrics (ATSPM) (Waddell et al. 2020; Waddell et al. 2020). Deng et al. use GPS trajectories to model intersections (Deng et al. 2018).

3. The framework for processing the raw ICV data

A big challenge of using the ICV data for transportation management is how to reduce the ICV data size to a manageable level for specific purposes. Due to the rich information and high resolution, even a few weeks of ICV data set will be hundreds of gigabytes or even terabytes of text files. They are beyond the capability of traditional data processing tools. To overcome these challenges, we propose a scalable data processing framework and filter irrelevant information from the raw ICV data and screen out the data irrelevant with the scope of studies. Also, we develop efficient map-matching algorithms to map vehicle GPS traces onto road links. Fig. 1 demonstrate the proposed ICV data processing framework.

3. 1 Step 1: data reduction for the scope of interest

The first core process in this framework is to reduce the data size and screen out irrelevant data set. The ICV data are often delivered in vehicle traces covering the entire area while the scope of congestion management only includes much smaller areas along the highways whose shapes are likely irregular. Checking whether geolocation points is within an irregular polygon at large scale is computing-intensive. To address this issue, we adopt an efficient approach proposed by Li and Li (Li and Li 2010). The data-reduction method due to Li and Li is to first convert vector GIS maps into raster maps and use each pixel's value to represent a link ID. In light of this idea, we first rasterize a broader bounding rectangle on GIS map. We only focus on the waypoints that are within the bounding rectangle. We then set all the pixels within the polygon of interest as one value that is different from those pixels out of polygon. Each waypoint within the bounding rectangle will be assigned the corresponding pixel value. At last, all waypoints are

grouped and filtered according to their assigned values. More details are provided as follows:

The congestion management is typically carried out for a city or a region within which the unit distances of longitude are viewed as constant (i.e., the city or region can be viewed as a flat plane). Therefore, we can safely map the vehicle GPS waypoints from the WGS84 coordinate system (latitude-longitude coordinates) into the local coordinates in a customized rectangular coordinate system.

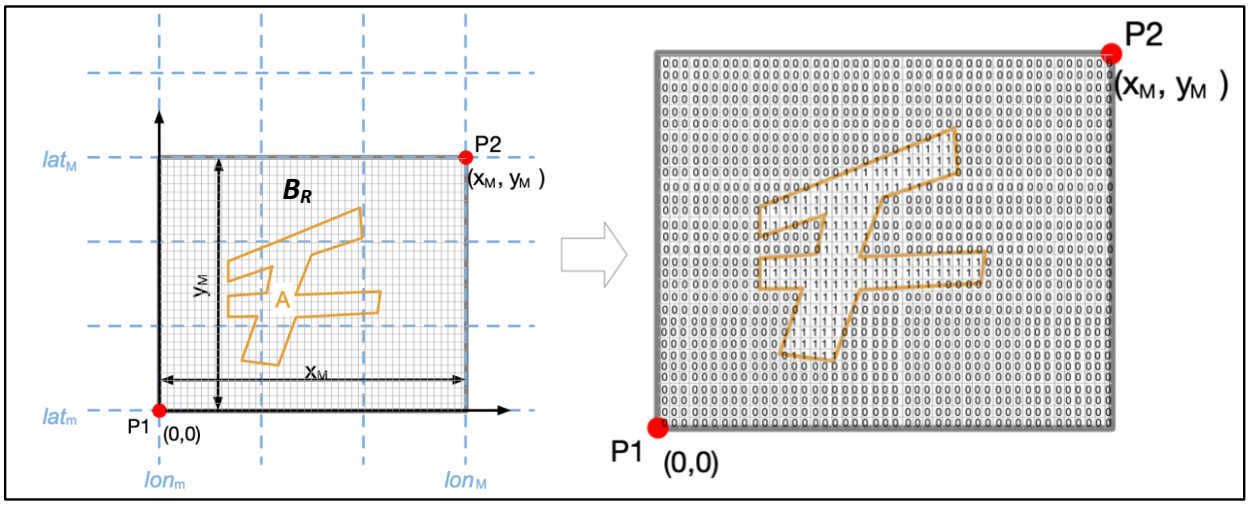

Figure 1 illustration of data reduction with the OpenCV library

As shown in Fig.1, the broader bounding rectangle, denoted as B_R, is first defined to cover all the road segments of interest. The irregular area of interest is denoted as A. The bottom-left corner of B_R is the origin with coordinates (0,0) in the local rectangle coordinate system, denoted as P_1. From an on-line map engine (e.g., Google Map), we can then find $P_1's$ latitude-longitude coordinates, denoted as (lon_m, lat_m). Secondly, the latitude-longitude coordinates of the top-right corner, denoted as P_2, is identified as (lon_M, lat_M). Thirdly, the rectangular B_R is further divided into $x_M \times y_M$ smaller cells. Using the cells as the units, then the local coordinates for P_1 and P_2 are$(0,0)$ and (x_M, y_M), $x_M \in$

$N^+, y_M \in N^+$. A larger x_M or y_M means a small cell size (i.e., higher resolution) along the x or y directions. The above conversion function from latitude-longitude coordinates(lon, lat) to local coordinates (x, y) in B_R can be formulated as:

$$(x, y) = F(lon, lat) = \left(\frac{x_M \times (lon - lon_m)}{lon_M - lon_m}, \frac{y_M \times (lat - lat_m)}{lat_M - lat_m}\right) \quad (1)$$

For each latitude-longitude point, (lon, lat), (1) will convert it into a local point, (x, y), in B_R.

With (1), the coordinates of polygon A' vertices, denoted as $\{(lon_i^v, lat_i^v), i \in \{0,1,2, \dots\}\}$ can be converted into the local rectangle coordinate system:

$$(\hat{x}_i, \hat{y}_i) = F(lon_i^v, lat_i^v) \quad (2)$$

To identify if a waypoint falls into A, the waypoint must be compared with all vertices of polygon A. This process, if carried out in sequence, will be time-consuming but can greatly speed up with advanced computing tools. In this context, since the proposed data-reduction process is similar with processing an image comprised of pixels, we adapt a computer-vision library, referred to as the *OpenCV*, to perform this process. We formulated this problem as a image processing problem.

We constructed a binary matrix, $\boldsymbol{M}$, with dimensions of $x_M \times y_M$. Each element represents a cell defined above in analogy of "image pixels" of B_R and A, and can be indexed by the row number i and column number j. Each element in $\boldsymbol{M}$ is initialized as "0" and those elements within A is then adjusted to "1". A function, M: $\mathbb{R} \times \mathbb{R} \rightarrow \{0,1\}$, can be constructed from the matrix $\boldsymbol{M}$. For a point, (x, y), within the B_R, the value of $M(x, y)$ is the value of the element in matrix $\boldsymbol{M}$ indexed by row $\lfloor x + 0.5 \rfloor$ and column $\lfloor y + 0.5 \rfloor$. For the points outside of B_R, the value is 0. This is described by Equation (3).

$$M(x,y) = \begin{cases} \left(\boldsymbol{M}_{\lfloor x+0.5 \rfloor}, \boldsymbol{M}_{\lfloor y+0.5 \rfloor}\right), & x \in [0, x_M), y \in [0, y_M) \\ 0, & o.w. \end{cases} \quad (3)$$

A latitude-longitude waypoint (lon, lat) will first be converted into the local coordinates (x, y) in B_R. We used the OpenCV library to mark down the corresponding latitude-longitude waypoints that are within A, i.e., $\{(lon, lat)|M(F(lon, lat)) = 1, \ \forall (lon, lat)\}$.The above data reduction process inspects each waypoint independently, allowing for parallelization. The GPS waypoints in this study are also delivered in multiple text files for each hour.

3.2 Map matching of vehicle GPS waypoints to time-dependent road link sequences

Traffic congestion is typically evaluated based on road segments. Therefore, it is critical to map the vehicle trajectories onto road links and convert vehicle trips to a time-dependent link sequences for quantitative analysis. For the real-world problems with the ICV data sets, the map-matching task often requires matching millions of vehicle GPS waypoints to tens of thousands of road links. As such, the map-matching algorithm must be designed in such a way that it can significantly reduce the matching space and can parallelize the tasks into multiple CPU cores or computer clusters. To meet these goals, we design the map-matching algorithm as follows.

Step 1: Grid the road network.

The purpose of gridding the road network into cells is to exclude those road links obviously irrelevant to a GPS waypoint. Figure 2-a demonstrates the grid road network in the Dallas-Fort-Worth region. If a waypoint falls into Grid X, the algorithm does not need to compare those links in Grid ***Y***.

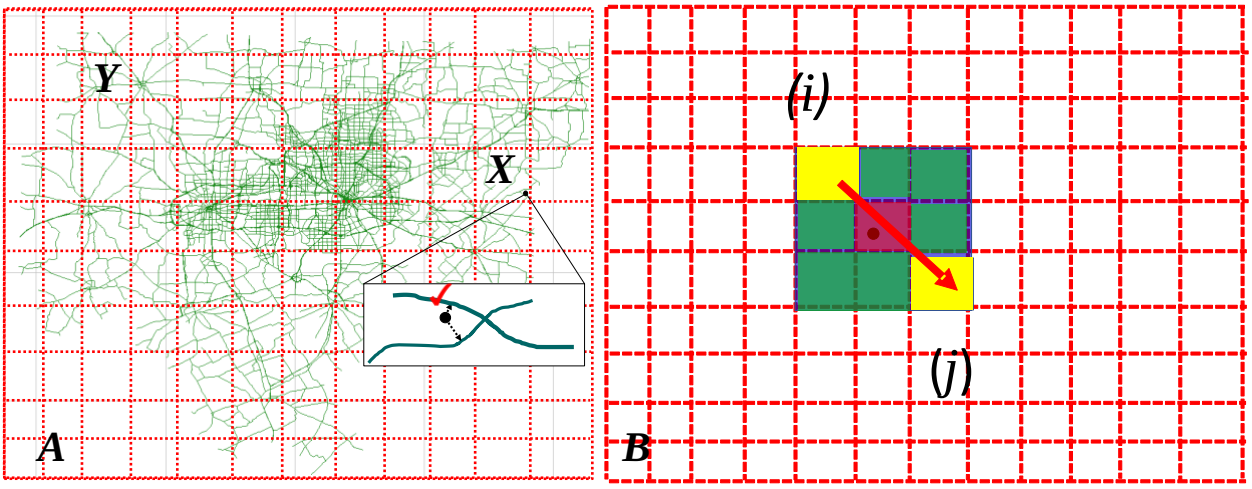

Figure 2 Gridding Road networks and map matching

Step 2: Identify the list of crossing grids for road links.

Regional highway networks are represented by nodes and links. After gridding the road network, certain long links (i, j), represented by two end nodes i, j, may cross more intermediate grids than just two grids. To ensure all crossing grids of a long link will be recorded, we extend the scope of long links. As illustrated in Fig. 2-b, Link (i, j) crosses three grids (yellow and red). We extend the list of crossing grids for (i, j) to all the grids within the shadow. This operation will guarantee any waypoint can always match its link even if the road network is sparse. The shadowed area in Fig. 2-b is an extended rectangle on the gridded road network to cover multiple grids (red, yellow and green). The rectangle uses two yellow grids as diagonal corners.

Step 3 Match GPS waypoints to links.

While matching a waypoint (e.g., Grid ***X***) to the road links, only those road links passing Grid **X** will be selected for matching and the link in the same grid with the shortest conjugate distance from the waypoint will be identified as matched link. (See Fig. 1)

After the map matching, each vehicle trip can be converted into a series of dynamic link sequence comprised of a link list and a time list. For instance, "$(l_1, l_2, \dots, l_n) + (t_1, t_2, .., t_n)$" represents that a vehicle enters link l_1 at t_1, leaves l_1 (i.e., enter l_2) at t_2 , leaves l_2 (enters l_3) at t_3 and so on. At this time, it is ready to analyze the link traffic performance based on the converted ICV data sets.

Remarks: Although Step 2 will ensure a waypoint will match the correct link, it also introduces unnecessary matching efforts. For instance, in Fig. 2, a waypoint in those green grids will have to calculate its conjugate distance to irrelevant link (i, j). Nonetheless, the long links crossing multiple grids is rare in the practical road networks. Therefore, Step 2 will not significantly increase the computing efforts.

Framework's scalability: Gridding the road network will dramatically reduce the number of links to be matched for each waypoint. Step 1 and Step 2 will jointly guarantee that the map-matching results will not deteriorate if the grid size is further reduced. Since the map matching for one waypoint is independent of other waypoints, the map-matching process for multiple waypoints can be parallelized on multiple CPU cores or computer clusters. Therefore, the proposed map-matching method is scalable, and it is suitable for large-scale problems.

Mismatching issue: A small portion of waypoints may be equally away from two links. For instance, while a vehicle is passing an overpass on freeways, its waypoints may be equally away from the freeway link and the overpass link. To avoid mismatching, it is necessary to examine the predecessors and successors of this waypoint within the same trip to ensure the correct links. Comparing the vehicle's heading (direction) with the road direction can also help remove the mismatching issue.

4. ICV-data-based performance metrics in time-space diagram

The time-space diagram (TSD) is a popular tool to reveal time-dependent traffic performance on roads. Since the ICV data ubiquitously cover all the locations with relatively large sample size. We can divide a road link into smaller segments to reveal the time-dependent traffic performance according to the ICVs' waypoints at different locations over time. The new performance metrics are designed according to the features of ICV data sets: time-dependent link speed map integrated with slow vehicle movements; degree of speed harmonization (DSH).

4.1 Time-dependent link speed map integrated with slow vehicle movements

Time-dependent travel speed: The time-dependent segment speed is calculated as the average speed of waypoints reported within each segment and time period.

$$\bar{v}_{t,l} = \sum_{i=1,..,n} v_{t,l}^{i} \quad (5)$$

Where: $\bar{v}_{t,l}$ is the average travel time on segment l during time-of-day period t; $v_{t,l}^{i}(i = 1,2, \dots n)$ is the reported speed in a waypoint within the segment and time-of-day period.

Vehicle slow movements and queue length: the slow movements are identified when a vehicle's speed has reduced below a threshold. When an internet-connected vehicle joins queue end at a bottleneck, its speed will significantly reduce. Therefore, we can estimate the propagation of queue lengths at bottlenecks according to when an internet-connected vehicle begins to report slow movements. As illustrated in Fig. 3, the start of a stable slow movement represents the instantaneous queue end at bottlenecks.

The proposed performance metric is a combination of travel speed and vehicle slow movements and it will be demonstrated in Case Study I.

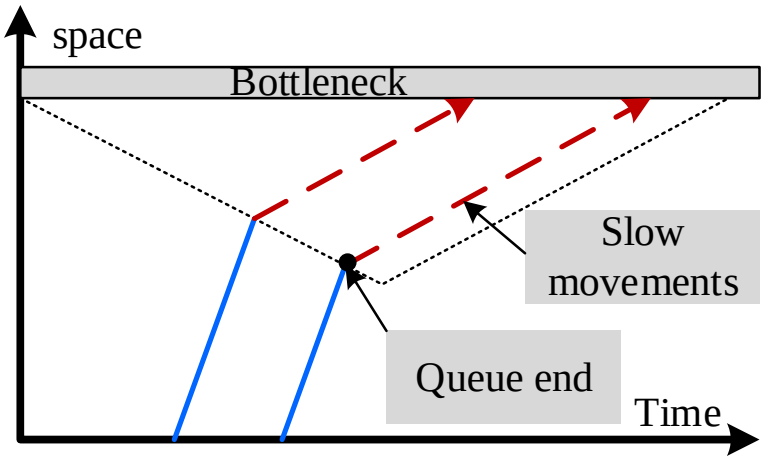

Figure 3 Identifying queue end with vehicle slow movements at bottlenecks

4.2 Degree of speed harmonization (DSH) on road segments

While the travel speed is a straightforward indicator of traffic mobility, it also averages out the heterogeneity and fluctuation of individual vehicles. As shown in the Fig. 4, vehicle 1 accelerates and decelerates multiple times between location i and location i whereas vehicle 2 only accelerates once. If we use the average speed to represent the two vehicles' maneuvers, then the vehicle 1's stop-and-go pattern will be missing.

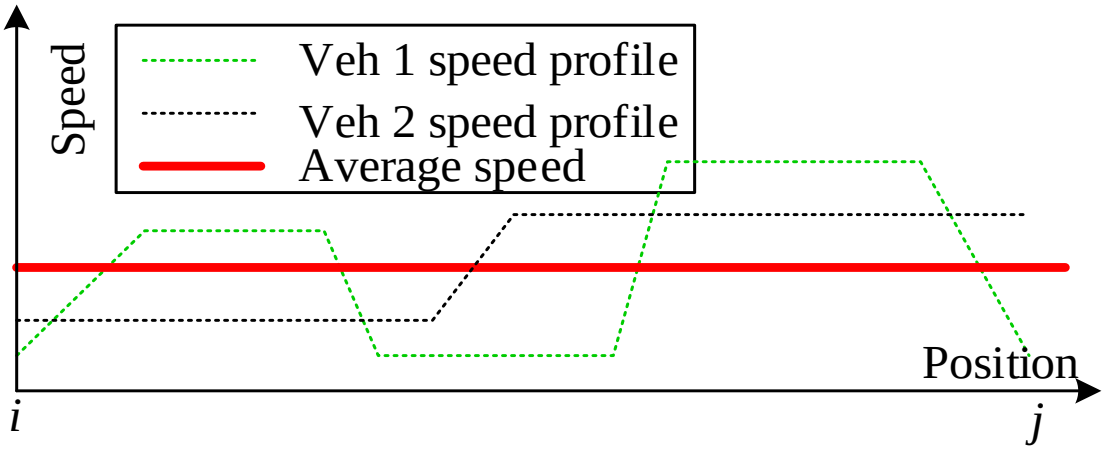

Figure 4 Speed files of two heterogeneous vehicles with the same average link speed

Since vehicles' stop-and-go characteristics directly reflects both traffic safety hazard and congestion, we propose the following performance metrics to reflect the speed harmonization on road segments.

Denote the collection of speeds of a trip p on a road link as $\{v_p^i\}, i = 1,2,\ldots..$ then non-negative speed change value and the average speed change of p are defined as $\{d_p^i\} = \{|(v_p^i - v_p^{i-1})|\}, i = 2,3,\ldots$ and $\bar{d}_p = \frac{(\sum_{i=1,2,\ldots n} d_p^i)}{n}$, respectively. The DSH on link l is calculated as follows:

$$DSH_l = \frac{(\sum_{p=1,2,\ldots m} \bar{d}_p)}{m} \qquad \text{for } \forall\, l \tag{6}$$

(6) shows the DSH of all vehicles on l during the study period. It is similar with the definition of "coefficient of variation" in statistics indicating the normalized deviation of a vehicle's reported speeds. DSH is related with traffic safety and vehicle emissions. The larger the dimensionless DSH of a cell is, the more likely vehicles frequently accelerate and decelerate, implying traffic safety hazard and vehicle emission issue.

5. Case study I: Using the ICV data to identify queue propagation at freeway bottlenecks

The queue length at freeway bottlenecks is traditionally estimated according to traffic counts at upstream and downstream locations. For example, Lawson proposes an approach to estimate the queue length based on the vehicle cumulative counts, also known as A-D curves (Lawson et al. 1997); Newell proposes a so called three-detector method to estimate the queue length at freeway bottlenecks (Newell 1993). However, these methods of queue length estimation are sensitive to the selected parameters (e.g., vehicle speed while moving in the queue). Using the ICV data, we can directly measure

the queue length and propagation at freeway bottlenecks. Through synthesizing multiple days of ICV data, we use the performance metrics proposed in Section 4 to identify the spatio-temporal characteristics of queue lengths at bottlenecks.

The selected freeway segment on I-20 interstate highway is one of major corridors for travelers within City of Arlington, Texas. There are also six ramps along the I-20 in Arlington, potentially causing vehicles to slow down. Following the framework proposed in Section 3, we first process the raw ICV data and only reserve relevant vehicle trips. A related vehicle trip is identified if at least one of its waypoints is located within the study scope and has a correct heading. In addition, a vehicle trip is broken into two or more if a time interval between two consecutive way points is longer than 2 minutes. In that case, it means the same vehicle may likely have taken off the mainline and then taken on the ramp again. Therefore, the same vehicle trip should be viewed as two separate trips. In the preliminary data screening, totally 36,345 vehicle trips were retrieved from June 1st, 2020 to June 7th, 2020. Using the processed vehicle trips, we then construct a 24-hour time-space diagram with multiple days of vehicle trips to identify spatio-temporal bottlenecks. The speed limit on I-20 in Arlington is 70 miles per hour (MPH). If a waypoint speed is lower than 40 MPH, a local empirical threshold, then the vehicle's waypoint is labelled as a "slow movement", suggesting that this vehicle is in a moving queue. Since the ICV waypoints cover the entire freeway segment, we further divide the freeway into several subsegments with 0.5-mile length to inspect the traffic performance metrics at each subsegments. Furthermore, we divide one day into 24 hours.

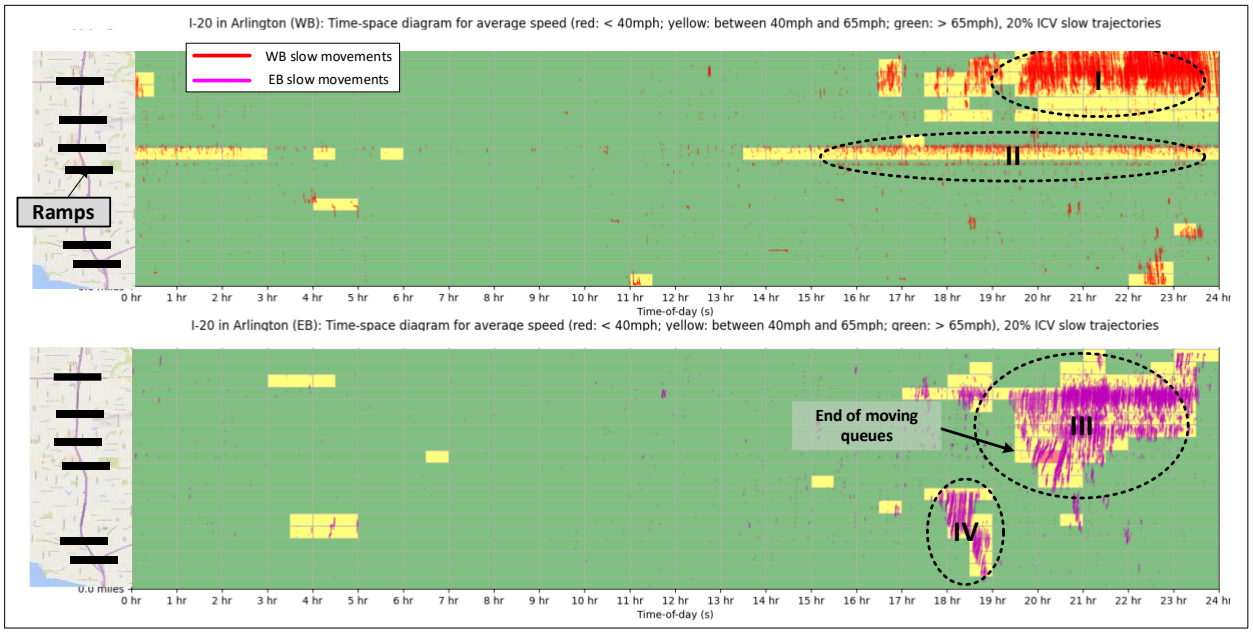

Figure 5 Time-space diagram of dynamic travel speed integrated with slow vehicle movements

Fig. 5 reveals high correlation between travel speed and slow trajectories. For instance, we can identify low-speed cells, such as those in Areas I, II, III and IV. We can also identify the queue propagation in those areas, too. The colored cells and slow trajectories jointly visualize the spatio-temporal characteristics of freeway bottlenecks. In particular the EB queue length in Area III, developed at a ramp, seems to have lasted a few hours and the queue propagated back to upstream ramps. The queue length reached the maximal between 8 PM and 9 PM and then disappeared after 11: 30 PM. Note that the ICV data for this case study were collected during the lockdown period of Texas. Therefore, there were no obvious morning and evening peak hours. The cause for the bottlenecks was the road construction and work zone management. The local agencies decided to speed up road construction projects during the pandemic because the traffic volumes dramatically decreased.

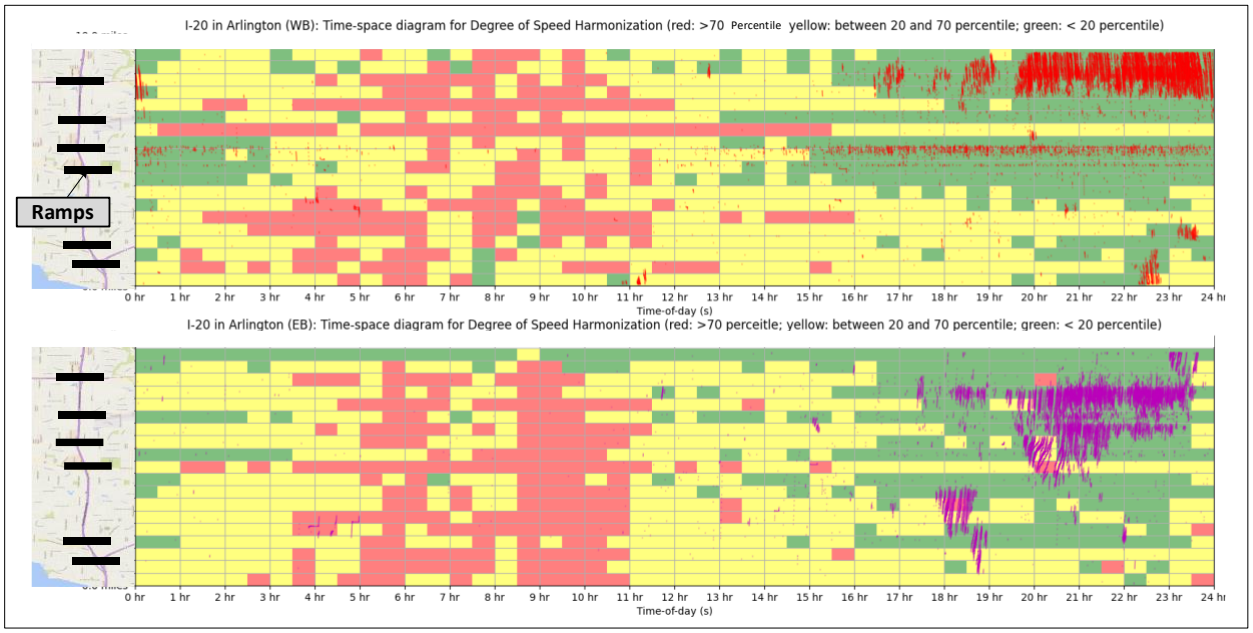

Figure 6 Time-space characteristics of degree of speed harmonization (DSH)

Fig. 6 reveals the DSH values in each cell. A three-color code is used to represent the DSH in each cell. We can tell that the DSH has low correlation with travel speed. Compared with the slow trajectories. It seems that vehicles DSH reduces after they slow down and join the queue. This makes sense because vehicles have less flexibility of speed changes due to the close spaces with other vehicles.

6. Case Study II: Using the ICV data and traffic control data to identify arterial congestion

Intersections on arterials are natural bottlenecks on arterials. Compared with freeways, the agencies typically collect various types of data via fixed-spot infrastructure detectors and traffic signal control events. Data-driven traffic control performance metrics is one of focuses of the “Every Day Counts Initiatives” program overseen by Federal Highway Administration (Wagner 2014). More recently, researchers begin to explore integrating vehicle trajectories with infrastructure traffic data to create novel traffic performance metrics. The most common method to reveal the arterial traffic bottleneck is the time-

space diagram (TSD). The TSD reveals the performance of traffic signal control across multiple intersections and the performance metrics include green bandwidth, maximum queue length, etc. Fig. 7 is an arterial time-space diagram based on traffic signal events (signal control records at each intersection) and vehicle trajectories (curves between intersections).

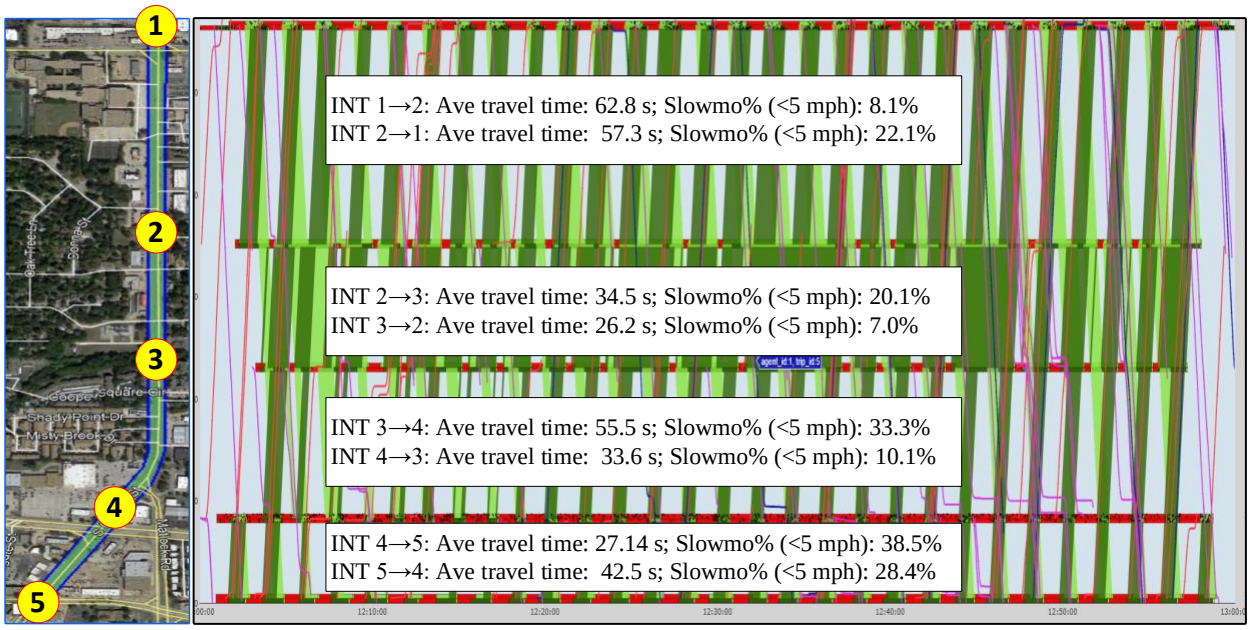

Figure 7 Arterial time-space diagram and mobile-sensor-based performance metrics

The high-resolution traffic signal events are footprints of traffic control operations. Whenever a traffic controller changes its status (e.g., capture an approaching vehicle, a green phase start or ending, etc.), this control event will be timestamped and archived. We can use the control events to construct the TSD using the control events. Constructing TSDs ideally needs both high-resolution traffic signal event data and synchronous vehicle trajectories with sufficient penetration rate, the latter of which are not available until recently. In this case study, we explore to combine the ICV data with the high-resolution traffic control log data and design new arterial traffic performance metrics based on ICV

data. The traditional TSD is solely based on infrastructure traffic data sets. Therefore, bias is likely introduced to reveal congestion under complex traffic conditions with queue spillbacks. The traditional TSD also assumes constant moving speeds between intersections unless vehicles join queues. This assumption may be also questionable because vehicles may slow down to enter a drive way, slowing down the following vehicles. Or vehicles may slow down and move in a two-way left-turn lane. These maneuvers cannot be captured by the infrastructure traffic sensors and so the TSD may convoy misleading information about arterial traffic performance.

The selected arterial is five consecutive intersections of the Cooper Street in City of Arlington, Texas. All the five intersections can archive high-resolution traffic signal events data. The speed limit on the Cooper Street is 40 MPH. Since the mainline green duration varies from cycle to cycle under actuated traffic signal control, it will be more accurate if the high-resolution traffic signal events and ICV waypoints are synchronized. By contrast, the freeway congestion can be evaluated solely with the ICV dataset. In the North America, most arterials are controlled by actuated traffic signal systems. A common mechanism in the actuated traffic signal system is “early return to green”, returning any unused green time allocated for minor approaches back to the mainline. As a result, the green duration on the arterial mainline may vary from cycle to cycle. In order to evaluate the high-fidelity delays, queue lengths, travel speed, etc. given, it is necessary to avoid averaging out the cycle-to-cycle differences. To meet these goals, we design an arterial time-space diagram based on the ICV trajectories and traffic signal events across multiple intersections. Other than the common travel speed or arrivals-on-green percentage described in other literature, we design a new performance metrics between two

consecutive intersections: the *percentage of slow movements* of vehicle trajectories. Using all the waypoints between two intersections during the study period, the slow movement percentage is calculated as:

$$p_s = \left(\frac{\sum_{i=1,..,m} v_i'}{\sum_{i=1,..,n} v_i}\right) \quad (7)$$

Where: p_s is the slow movement percentage; v_i' is the waypoint speed which is lower than a threshold (e.g., 5 miles per hour); v_i is the waypoint speeds; m: the number of slow speeds; n: the number of total waypoints.

Compared with the link travel speed, an advantage of the slow movement percentage is that it can reflect the vehicles' actual queuing time between intersections. The link delay is defined as the actual travel time minus free-flow travel time. In practice, vehicles' moving speeds are seen different from the speed limit. Therefore, the averaged link delay time may misestimate the actual queuing time. In Fig. 8-A, t_1 is the reported link delay while the vehicle's actual delay time is $t_2 + t_3$ and it is greater than t_1 because the vehicle's desired speed is faster than the free-flow speed. Fig 8-B demonstrate the other possibility, $t_2 + t_3 < t_1$ because the vehicle's moving speed is lower than the speed limit. The driving experience, energy consumption and emission are more sensitive to low-speed maneuvers. Identifying the actual queuing time accurately is important to evaluate the traffic signal performance and vehicle energy consumptions on arterials. To address this issue, the slow movement percentage is designed to capture the real delay time between intersections, which is critical to estimate the control delay given a traffic signal timing. The aggregated average travel time and slow movement percentages (speed<5 MPH) between intersections are shown in Fig. 7, which is generated according to the ICV data (trajectories in the TSD) and high-resolution traffic signal events (mainline traffic

control status and green band) from 12 PM to 1 PM on Dec-29-2020. The actual delay time is calculated as average travel time multiplied by slow movement percentage.

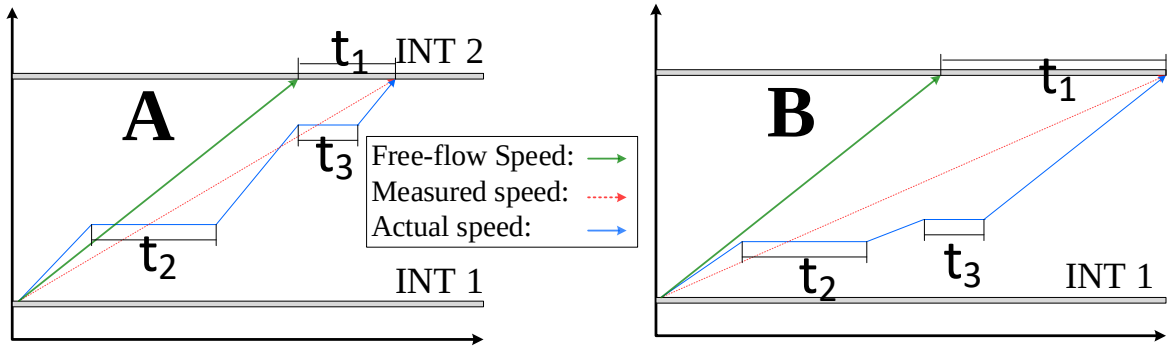

Figure 8 Using slow movement percentages between intersections to calculate vehicles' actual delay time (when speed < 5 MPH)

7. Conclusion

In this paper, we present our efforts in exploring and exploiting the potential internet-connected vehicle (ICV) data set. The ICV data are passively crowdsourced from the on-board positioning and communication modules in recently manufactured vehicles. The raw data from the distributor, the Wejo Data Service Inc. are well organized but have super big volumes. Therefore, we first design efficient algorithms to screen the data set and match the vehicle waypoints to the maps. We further design two new traffic performance metrics and their visualizations in the time-space diagrams based on the characteristics of ICV data sets. One case study is conducted on the interstate I-20 in Arlington, Texas and the other case study is conducted on the Cooper Street in Arlington, Texas in conjunction with high-resolution traffic control events from the infrastructure. The Cooper Street is a major arterial in Arlington. The features of the proposed traffic performance metrics include that: (I) we can identify the queue propagation at freeway bottlenecks, based on where and when most internet-connected vehicles began to

considerably slow down and joined the queue; (II) we can identify a vehicle actual queuing time between intersections based on its slow movement percentage. The new performance metric does not need to assume a non-delay travel time. More accurate estimation of vehicles' queuing time is critical for traffic signal timing design and the estimation of vehicles' energy consumption. Based on the above findings, we conclude that the ICV data set has a huge potential in enhancing traffic congestion management planning both on freeways and arterials.

8. Acknowledgement

This research is partially supported by the project "Exploring a Novel Public-Private-Partnership Data Sharing Policy through a collaborative Arterial Traffic Management System" sponsored by the USDOT UTC Center, Center for Transportation Equity, Decisions, and Dollars (CTEDD). The ICV data are distributed by Wejo Data Service Inc. Any opinions, findings, conclusions, or recommendations expressed in this material are those of the authors and do not necessarily reflect the official views or policies of the above organizations, nor do the contents constitute a standard, specification, or regulation of these organizations.

PART II

Evaluating the Impact of Emergency Vehicle Preemption Strategies on a Smart Signalized Corridor Using a Microscopic Simulation Model

Somdut Roy

School of Civil and Environmental Engineering

Georgia Institute of Technology

788 Atlantic Drive NW

Atlanta, GA 30332, USA Tel: 678-602-3220 Email: somdut.roy@gatech.edu

Michael Hunter, Ph.D.

School of Civil and Environmental Engineering

Georgia Institute of Technology

788 Atlantic Drive NW

Atlanta, GA 30332, USA

Tel: 404-385-1243 Email: michael.hunter@ce.gatech.edu

Angshuman Guin, Ph.D.

School of Civil and Environmental Engineering

Georgia Institute of Technology

788 Atlantic Drive NW

Atlanta, GA 30332, USA Tel: 404-894-5830 Email: angshuman.guin@gatech.edu

1. INTRODUCTION

With recent advances in the pilot testing and deployment of Connected Vehicle (CV) technologies (*1; 2*), there is a massive surge in the quantity and quality of data that is becoming available for aggressive feedback into real-time operations of transportation management systems, especially signal systems. Among the wide swath of applications proposed as CV technology, advancement of Emergency Vehicle Preemption (EVP) is one that is ripe for implementation, as it targets a specific set of vehicles and does not require a substantial penetration of On-Board Units in the general traffic.

EVP is not a new concept and has been used in the past with varying levels of reported success (*3-5*). The benefits of EVP have been somewhat restricted in the past, especially in congested roadway conditions, because of the line-of-sight requirement between the EV transmitter beacon and the preemption request receiver at the traffic signals. However, there have been recent technological developments in this space with the integration of GPS device based triggering mechanisms for preemption (*6-9*). CV technology provides a seamless means to integrate live vehicle position and multiple intersections' signal status data-streams, enabling enhanced strategies for optimal EVP performance. With Emergency Vehicle (EV)'s on board CV equipment and CV roadside units (RSUs) connected to the signal controllers, the line-of-sight restriction is no longer required. This opens up the possibility of creating a free-flow path through the signalized intersections for the EV. By anticipating the arrival of the EV, based on its position as recorded by CV messages received at other RSUs in the system, vehicles on the approach of interest may be cleared before the EV arrives. While such a methodology has been proposed before, and has seen limited implementation using GPS and cellular-

phone based technologies, there is not sufficient literature on clear before-after evaluations of a distributed predictive EVP implementation. Research is also limited on the methodology of implementation.

This paper develops a methodology for evaluating different EVP strategies made available through CV technology. Additionally, while EVP reduces EV travel-time delays, it may negatively impact the flow of the general vehicles at the given location or corridor. This paper develops a simulation model for a roadway corridor in Georgia and evaluates the impact of EVP on both EV performance and general traffic. While the EVP strategy that minimizes emergence vehicle travel time should be selected it is possible the strategies with similar EV performance may have different impacts on the general traffic. By way of example, this paper studies the impact of two different strategies for returning the signal operations to normal operation after an EVP actuation and evaluates the recovery process by measuring the effect on the travel-times of the vehicles on the mainline as well as the vehicles on the cross-streets.

2. BACKGROUND RESEARCH

This section provides a brief introduction to EVP and provides a summary of previous studies relevant to this research. Per MUTCD 2009 Edition (*10*), traffic signal preemption is defined as the change in operation of a traffic signal from normal mode to a special control mode. The primary objective is to give a certain class of vehicle hindrance-free passage by providing a green indication for the route of the said class of vehicle. Preemptive control can be given to trains, boats, EVs, and light rail transit (*11*). EVP is the phenomenon of preemptive operation intended for EVs, such as firetrucks,

ambulances, etc. with an aim to give right-of-way to the vehicle, minimizing the delay in reaching the incident location (*12*). The preemption triggering message can be conveyed to the signal cabinet through a multitude of methods; the driver could externally relay the message (by use of strobe, siren, pushing buttons, etc.) or the infrastructure could be equipped to sense EVs through pavement loops, radio transmission, or other vehicle to infrastructure (V2I) technologies (*11*).

The primary purpose of extending green time in EVP is to reduce the travel time of the EV and ensure a safe and clear pathway for the vehicle (*13*). The preemption process involves two transition phases, one going into the preemption state, and the other coming out of preemption to restore normal signal operations. The Traffic Signal Timing Manual (*11*) states that, both the transitions, the yellow and all-red intervals shall not be shortened or omitted. Other guidance for transitions is include for pedestrian timing, returning to a red indication, allowable indication transitions, and accounting for multiple preemption requests.

Several studies on evaluation of EVP considered the delays experienced by the opposing approaches along with the EV travel time reduction. Nelson and Bullock (2000) focuses on investigating the effect of preemption calls on traffic congestion (*14*). The case study was performed in a simulated environment by linking a model built in TSIS/CORSIM to the signal controllers using Hardware in the Loop Simulation (HILS) technology. SR-26 in Lafayette, Indiana was simulated as a network having seven preemption paths with 1-3 preemption calls made in a predetermined time duration. For the phase transition, three algorithms *smooth*, *add* and *dwell* were studied and it was inferred that the smooth transition algorithm worked best in most cases. While studying the effect of EVs, the study

found that for both arterials and side streets, having a single preemption call in the simulation period had little to no effect on the overall travel time and delay. Ten, Hualiang, et al. (2003) studied the amount of disruption of coordination signals using microscopic simulation models based on multiple locations of New York City. For this study, the EVP related disruption took a maximum of four signal cycles to recover (*15*). Xiaolin and Khan (2012) used MATLAB simulation to study the effectiveness of two control strategies for EVP to reduce response time and effect of the EVs on general traffic. The study suggested the use of a predefined "notification time period" for the network to design an algorithm to maximize the improvement for EVs while minimizing the adverse effect of preemption on side streets. There were several other studies (*16; 17*) that tried to solve this delay tradeoff. Homaei et al. (2015) used fuzzy logic to select the preemption phase and extend the green time based on demand and queue length using available V2V and V2I technologies (*18*). Other studies approached this problem from the network path perspective, as a route planning problem (*19-21*).

The existing literature shows that it is imperative that a study of the impact of EVP accounts for travels time both on the route of the EV as well as the routes that are interrupted. There have been previous studies on the evaluation of innovative algorithms to optimize EVP performance and traffic disruption. However, these studies typically studied preemption at a single intersection or a few non-contiguous intersections in a small network. This paper studies the EVP problem on a medium sized network (with 25 intersections) using preemption on 8 contiguous intersections to specifically focus on the problem of disruption of signal coordination. The study also uses additional data available from a limited deployment of CV technology (with on-board-units on EVs and road-side-

units at intersections) to feed a “Dynamic Preemption” logic to optimize the movement of the EV through the intersections.

3. MODEL DESCRIPTION

This paper uses a microscopic simulation model of a corridor to evaluate different EVP strategies and their effectiveness in providing the shortest travel-time for the EV while keeping the delays experienced by the remaining traffic at a minimum. A simulation approach was chosen in favor of a before-after study given the advantages of rapid evaluation of multiple scenarios facilitated by a simulation environment. A microsimulation model build on PTV’s VISSIM 2021® (*22*) was used for this study. Replicate runs are made efficiently using Python 3.7 (*23*)’s scripts to drive VISSIM® using its Component Object Model (COM) module.

4. Study Site and Data Description

The simulation model is built for a 6.2 mile stretch along the Peachtree Industrial Boulevard (PIB) corridor from Holcomb Bridge Rd at the south-west end to Pleasant Hill Rd on the north-east end, in Norcross, Georgia. The model includes 25 intersections on and around the major road. The layout of the network in PTV VISSIM® and the network extents in satellite view are represented in **Figure 8 (a) & (b)**. For consistency, PIB is referred to as a North/South corridor throughout the length of the corridor. The cross-street approaches are defined as Eastbound (EB) and Westbound (WB). For this model, the system entities, consisting of the network geometry and the signal-heads, were built based on satellite imagery from OpenStreetMaps™ (*24*).

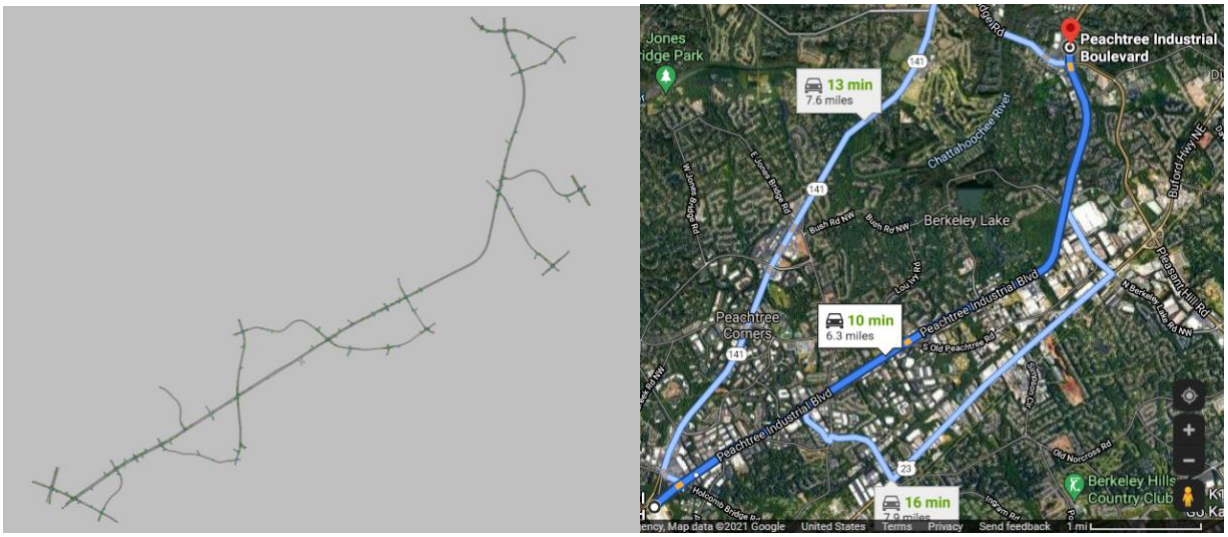

(a) **(b)**

Figure 8 Case Study Network of Peachtree Industrial Boulevard: (a) VISSIM® Simulation Model, (b) Satellite View by Google Maps™ (*25*).

5. Data Sources

The study focused on investigating strategies for preemptions during the 5PM-6PM peak hour, typically the most congested period for this corridor. For any day specific information the inputs defaulted to using data from a “non-holiday” weekday, Tuesday, October 01, 2019. Signal plan information was obtained directly from the field controllers, representing the active plans. A pre-COVID pandemic time period was chosen for the input data to ensure that the traffic and signal plans in the model represented typical traffic operations. VISSIM®’s Ring Barrier Controller (RBC) add-on module was used to simulate the signal controllers and preemption strategies. The obtained signal timing information was used as input to the RBC modules. The signals along the corridor are coordinated, with a 160 second cycle.

A single, comprehensive volume study was not available for this corridor. Thus, for the major and minor road approach volumes, data was assimilated from multiple sources including short-term historical turn-volume count data, counts obtained from post-

processing presence detector activations, recent traffic studies on the corridor, any available Automated Traffic Signal Performance Measures (ATSPM), etc. The signals on this corridor are also connected to a central server where the high-resolution signal phase and timing data as well as detection data is archived. The archived data had the vehicle on-off pulse information corresponding to the detectors. Typically, inductive loop detectors upstream of the stop-bar at intersections, in pulse mode, that fed the detection were present only for the major road approaches and only for the through lanes. The pulse data was post-processed to generate vehicle detection data for additional volume calibration. Finally, volume balancing and volume constraint computations based on signal cycle allowance and roadway geometry were used to generate estimates to fill gaps in available data to create the input volumes for the model

To allow for a warm up period, the network is provided with 50% of the volume for the first 15 simulation minutes. Then the volume is raised to 100% for the next 75 simulation minutes. Of the total 90 simulation minutes, data from the first 30 minutes are not used for collecting any simulation results to allow for a simulation saturation period. The last 60 minutes are used for collecting results to generate performance metrics corresponding to the 5PM to 6PM time period.

6. MODEL CALIBRATION

Model calibration by adjusting model parameters to maximizing the agreement of the model behavior to field observations (*26*) is an essential step to ensure that the model follows the travel behavior of the network that is being modeled. While fine-tuning the key parameters of the model to mimic real traffic in the network is necessary, it is not always possible to match the exact scenario of traffic vehicle-to-vehicle. Nor is that desirable as

it that could lead to an overfitting problem that could affect the robustness, translatability, and generalization of the results. In this study, the calibration effort ensured that the model sufficiently reflected the field conditions. Subsequent validation tests with travel-time as the performance metric were performed to confirm the sufficiency of the calibration.

6.1 Model Calibration I: Speed

Free-flow speed is one the key-features defining the traffic flow of the network. For determining the free-flow speed on the major road, GPS data collected on the corridor was used. GPS data collection equipment was deployed on 17 Fire Station Vehicles, belonging to six different Fire stations around the corridor, including a mix of Ambulances, Fire Engines, and Fire Trucks. This dataset provided high resolution (2-second updates) probe vehicle data in and around the PIB network. The data was fused with the emergency response logs pertinent to these vehicles to separate trips where the vehicle was in emergency-response mode versus a return-trip mode. To avoid any unusual driving behavior, only data-points with the “Flashers OFF” mode were considered for the analysis. The trips in the return-trip mode were used to represent driving behavior under normal conditions and were used to determine the free-flow speed distribution. The overall speed-histogram is subjected to a deconvolution process to extract the data-points representing the free-flow speed in the network. The deconvolution process followed the methodology developed in a previous study by Anderson et al. (*28*). The distribution with the highest mean was chosen to represent the free-flow speed distribution; a Normal distribution with (Mean: 52 mph, SD: 8 mph).

6.2 Model Calibration II: Headway

The other parameter that is crucial for model calibration, pertinent to this analysis, is saturation headways (*29*). The count detectors on the major road approaches were used to measure headways by recording the gap between two “Entry” pulses for a detector. To avoid sparse traffic overly affecting the headway distribution the headway measurements were limited to observations less than 4 seconds. Similar to field detectors, 6 ft pulse detectors were placed in the VISSIM® model at the corresponding locations to the field detectors to obtain the corresponding headways in the model. To calibrate the VISSIM headways with those from the field detectors, the car-following parameters under VISSIM®’s *Wiedemann 74* model were modified (*27*). Two key parameters of *Wiedemann 74* that dictate the headways are the additive part and the multiplicative part of the safety distance. The additive part dictates the average headway and the multiplicative part dictates the spread of the headway distribution. Four random seeds of VISSIM simulation results were compared to four weekdays of field detector data. For example, as shown in **Figure 9 (b)**, approximately 1175 data-points per VISSIM simulation were compared to approximately 1400 data-points/day of field detector data at the NB approach of PIB at the Medlock Bridge Road intersection. The average headways (as depicted by the dotted vertical lines) for the field (labeled as MaxView) and VISSIM after calibration lie very close to each other, in the 2.3-2.4 seconds range. The Cumulative Distribution Function (CDF) lines, shown as the orange and blue monotonically increasing lines, are also similar. A *two-sample Kolmogorov Smirnov (KS) test,* a non-parametric statistical hypothesis test,

performed on the two distributions concluded that the null hypothesis “the headway data sets come from the same distribution” cannot be rejected at a 90 percent confidence level.

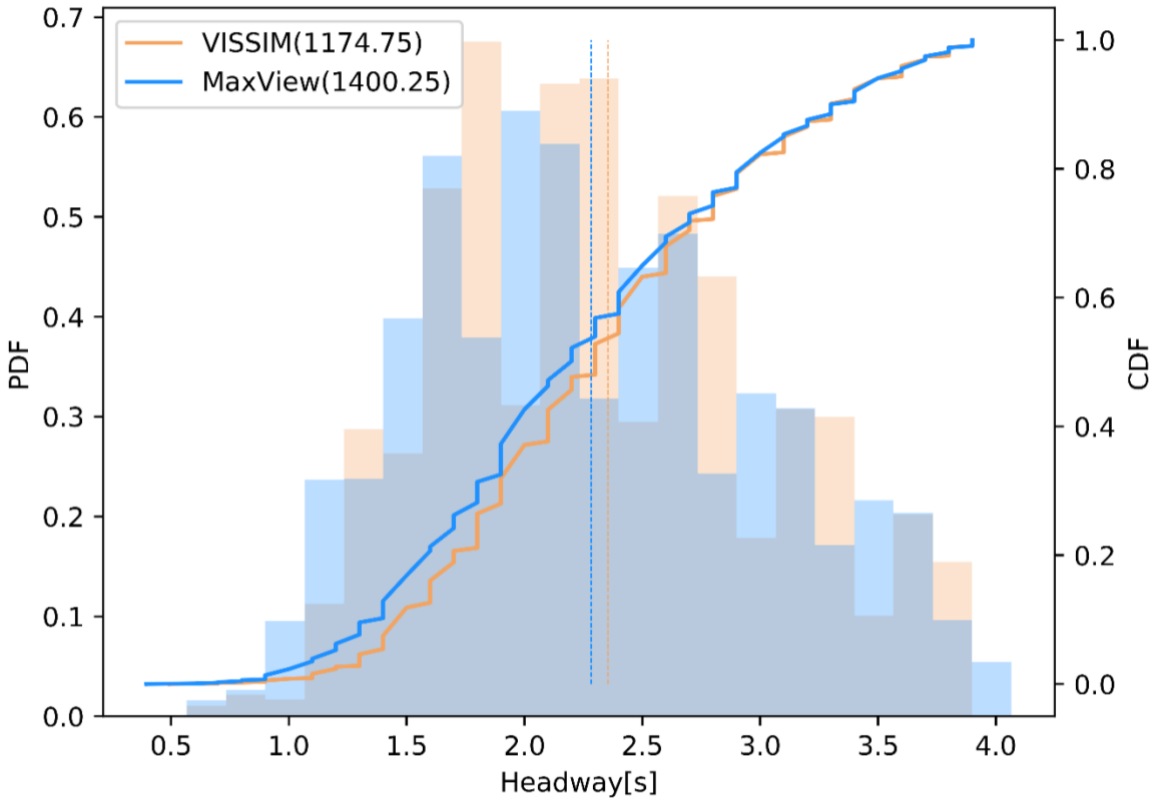

(a) **(b)**

Figure 9 Calibration Results: Headway Distribution for Northbound (NB) Movement at PIB@Medlock bridge Rd: MaxView vs VISSIM

As a final calibration step minor changes were made to the signal timing splits and vehicle extension timers at several intersections to better serve the synthesized traffic volumes.

6.3 MODEL VALIDATION: TRAVEL TIME

With the car-following and free-flow parameters calibrated, it is important to check how closely the traffic in the model behaves compared to real world. For model validation, travel-time was used as the performance metric. The traffic on the PIB corridor is directional with the PM peak traffic direction being north; additionally, the later EVP study,

will focus on the NB direction of travel. While this discussion will focus on NB travel, a similar process was undertaken for the SB direction with acceptable travel time performance.

Checkpoints were placed at two intermediate points on the NB PIB route to divide up the corridor such that sufficient complete vehicle traces could be captured for the travel time computation. The average travel time at the checkpoints were summed to determine a total average travel time for the entire 6.2 mile stretch of NB-through route along the PIB. As a benchmark, weekday travel time data from (a) theRegional Integrated Transportation Information System (RITIS) (*30*) and (b) Google Maps™ (*25*) [recorded at 5-min intervals during the 5-6 PM period on July 16, 2021] were used. The average RITIS travel time was 960 seconds, while Google Maps travel time averaged at 825 seconds. The travel time derived from the model came out to an average of 899 seconds. As per criteria set by Federal Highway Authority (FHWA)'s Traffic Analysis Toolbox (*29*), the simulated travel time should be within 15% of the field. The travel time in VISSIM lies within 15 percent of either of the data sources and satisfies the suggested validation criteria.

7. EXPERIMENT DESIGN

Once the baseline model calibration was completed, experiments were designed to study the impact of preemption on:

a. EV travel-time,
b. Travel-time of passenger cars on the mainline, and
c. Travel-time of passenger cars on the side-street.

The experiment studies the impact of EVP on a 45-mph speed limit signalized road during a period of heavy demand, especially on the NB route. The impact is evaluated with respect to strategies that address both the transition of the signal from normal operation to preemption operation and the transition from preemption operation back to normal operation. For the transition into preemption, an algorithm for flexible timing of the start of the transition is developed, rather than utilizing a fixed time or distance offset as typically deployed in the field. For the transition out of preemption a *normal* exit with service of the phase following the preemption phase in a normal cycle, is compared with an *in-step* exit where the preempt exits into the coordination pattern of the signal cycle. For this study, an EV must pass through an intersection during a green utilizing lanes in the correct direction of travel. That is, simulated EV behavior does not allow for running a red or passing through the intersection in the lanes of the opposing traffic. For each simulation run a single preemption event is modeled.

8. Entry Transition

VISSIM® allows external models for EVs, with specific geometry resembling a “firetruck” (*31*). One such model was used to create a vehicle class that was used for the preemption exercise. Presence detectors across the network are enabled so as to detect the presence of *firetrucks* selectively and the RBC controllers are programmed to enable preemption when the presence detectors are in an active state.

To improve the performance of preemption, using real-time data available from field detectors and the CV infrastructure, a “dynamic preemption” (DP) algorithm is devised. In this algorithm, the queue-length of an intersection is monitored from the time the firetruck begins to approach the upstream intersection. Based on the queue length, a

decision is made about how far ahead in time the preemption needs to be triggered so as to ensure that not only does the firetruck avoid entering the back of a queue, it also goes through the intersection without having to slow down. Thus, a sufficient time must be allocated for the vehicles in the queue as well as those in between the tail of the queue and the firetruck to clear prior the firetruck arrival. Some transition time is also allocated for the signal controller to serve the current phase yellow, red-clearance, and any necessary in-progress pedestrian-walk phases. Thus, the preempt call time is calculated as follows. If “n” cars are present in the queue, assuming that the headway is 2 seconds and an additional reaction time (i.e., start-up lost time) of 4 seconds, the time taken to clear that queue would be *(4+ 2*n)* seconds. It is also assumed there are vehicles between the end of the queue and the firetruck that need to be cleared, so an additional *2*n* seconds are taken. This is readily acknowledged as a rough estimate, which should receive field fine tuning. Additionally, as the vehicle fleet becomes increasingly instrumented with CV technology, real-time data may be used to better estimate this additional volume. For the transition from current signal state to the preempt phase, another *5* seconds are taken. This results in an overall total of *(9+4n)* seconds for the advance placement of the EVP call prior the firetruck reaching the intersection. Therefore, in a corridor with a free flow speed of “v”, the preemption will be triggered at a distance of *(9+4n)*v* from the intersection, when the intersection in question has a queue length of *n* cars.

In the simulation environment, the queue lengths were available as an output from the model. However, it is important to recognize that in a field deployment, the queue length will be an estimate rather than an observation. The queue length and the number of non-

queued vehicles ahead of the firetruck will be estimated based on the real-time detector data from the current and upstream intersections, or from the location information in the Basic Safety Message from CVs (with sufficient penetration of CVs). This estimation is a non-trivial problem, and has been studied by other researchers (*32; 33*). It is not discussed in this paper for brevity.

9. Exit Transition

While the entry transition has a significant impact on the EV's travel-time, the travel-time of the other vehicles are affected by the exit transition as well as the entry transition. With the default preemption algorithm in VISSIM®, the controller serves a defined set of exit phases or the next phase immediately after the preempt-phases, if no exit phase is specified. If a coordination plan is in place VISSIM® would then need to adjust the local cycle and splits to transition back into coordination. This is termed as *normal* exit in the VISSIM® RBC. Another possible option for the exit transition is *in-step*, in which the preempt exits into the coordination pattern of the signal cycle (*34*). In this exit transition, VISSIM® will exit into the current phase that would be running according to the local cycle, if sufficient time exists to serve the minimum green. If sufficient time does not exist it would exit into the next phase in the cycle, if a call exists. Finally, it will exit into the coordinated phase if the prior conditions are not satisfied. Underlying this logic is that no additional transition will be required to return to coordination.

10. EV Routes

To ensure that the effect of the signal coordination, or rather the disruption thereof, is investigated in sufficient detail, the EV routes were chosen such that they passed through multiple preempted intersections along the coordination path. The GPS data from the EV collected as part of the effort was used to observe historical travel patterns and ensure that the path chosen was representative. The path chosen is shown in

Figure 10 (a), **(b)**, and **(c)** as a series of historical GPS points, on a map and as part of the model network in VISSIM®.

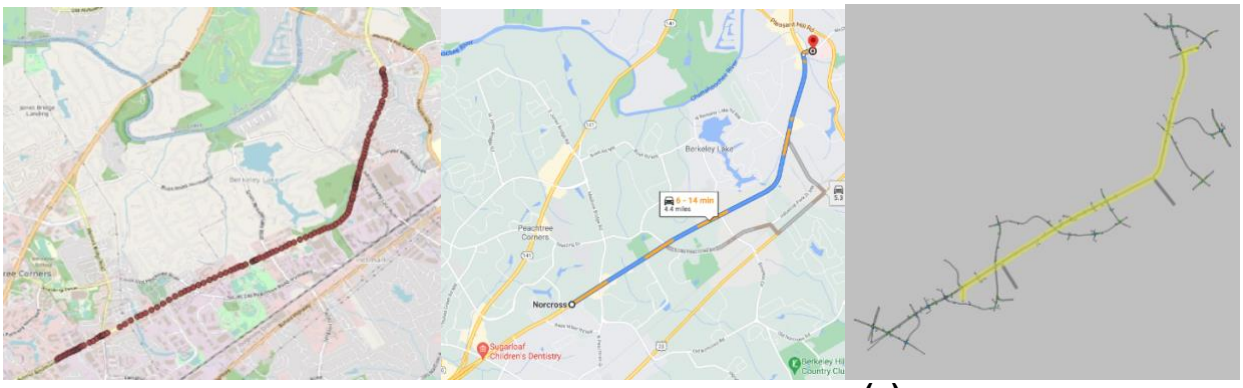

(a) **(b)** **(c)**

Figure 10 The NB Firetruck Route chosen for the Study (a) Actual Firetruck GPS data: OpenStreetMaps™ (24), (b) Route on Google Maps™, (c) Static Routing Decision in VISSIM® simulation model.

To summarize, the experiment consists of an investigation of three preemption strategies, (i) Preemption with *normal* exit, (ii) Preemption with *in-step* exit, and (iii) No Preemption. The “no preemption” case is treated as the baseline. Each of the 3 cases had 32 scenarios with different firetruck injection times, with 5 replications each, resulting in a total of 480 runs across all cases, scenarios and replicates.

11. RESULTS

11.1 Impact of EV arrival time

Prior to considering the three preemption strategies above, a brief analysis is conducted to understand the impact of a request for preempt relative to the local cycle time. It expected that that the time at which a firetruck makes a preemption request, relative to the local cycle and coordination plan, is likely to affect the entry into and exit from preemption and the associated impacts on the traffic. This effect is explored by introducing a firetruck into the network at different simulation times in an effort to touch different points of the signal cycle of the first intersection (PIB at the Medlock Bridge Road) in the route given in

Figure 10. As the cycle lengths of the signals are 160 seconds, 32 different scenarios are created, with a successive five second increment in the time of introduction of the EV into the network. To account for stochastic variability into the simulation, the exercise is performed using 5 random seeds. So, a total 32*5=160 simulation runs were conducted. For these runs, *normal* exit transition is utilized.

Figure 11 (a) & (b) shows the effect on the side-streets through movement travel times at the first preemption-activated intersection of PIB at the Medlock Bridge Road intersection. The impact is measured from the preemption event to two cycles after the end of preempt. In each successive scenario (shown along the x-axis) the firetruck entrance into the network is staggered by 5 seconds, which does not necessarily correlate directly with a specific part of the original signal cycle (before preemption), but does ensure sufficient variability such that arrivals are distributed throughout the cycle. It is

seen that the time of the preempt call relative to the local cycle may have a significant impact on the side street experience. As a sign of variation in mean travel time with firetruck arrival time, the mean travel time per scenario was observed to have a range of 63 s and 51 s on the EB and WB through movements respectively. Another way of understanding this scenario-based distribution is the difference between the 25th and 75th percentiles, also termed as the inter-quartile range (IQR). IQR dictates the amount of spread for the middle 50 percent of data-points around the median (*35*). It was observed that the IQR for travel time spanned between wide intervals of [80 s, 195 s] and [76 s, 176 s] on the EB and WB through movements, respectively.

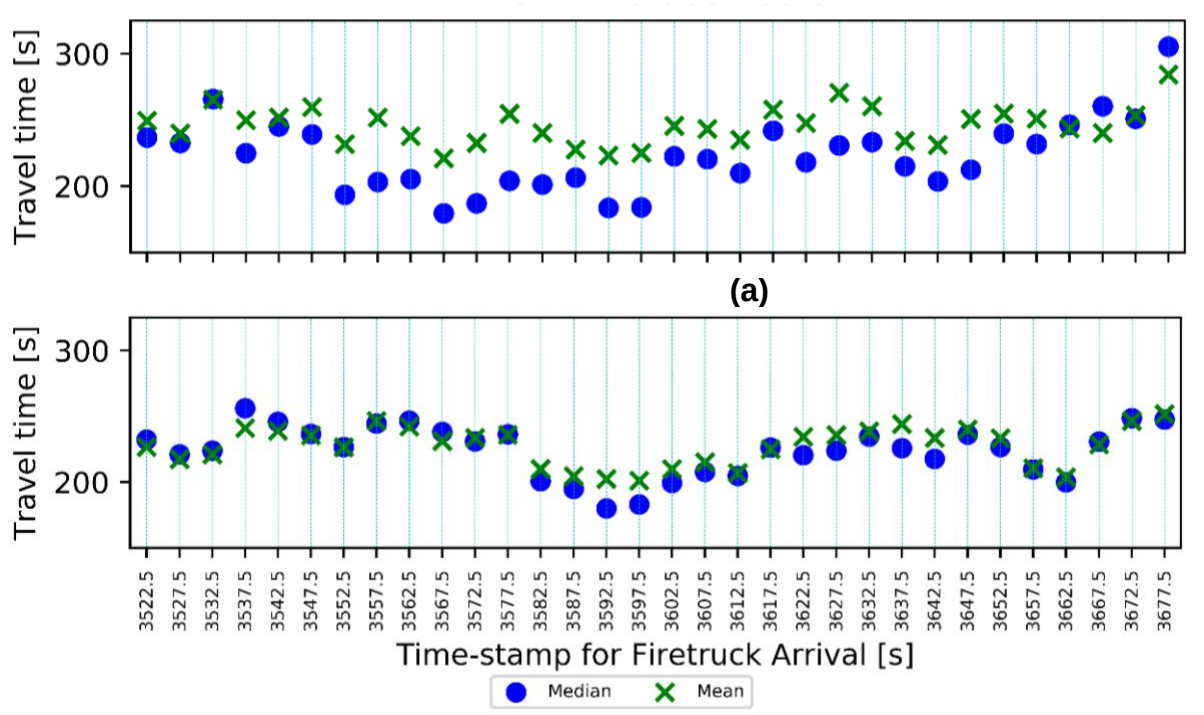

Figure 11 Variation in Travel Time for side-street through movement (PIB @ Medlock Bridge Road) for (a) EB Through and (b) WB Through with Different Firetruck Arrival Times.

The effect of the staggered entries on the travel-time of the firetruck (traveling the length of the corridor) is shown in **Figure 12**. Again, significant variability is seen, with the range

of mean travel time across scenarios at 42 s, while IQR spanned in the interval of [8 s, 99 s]. Given the range of variability seen, all subsequent experiments include sampling over the range of potential preempt call placements throughout the cycle.

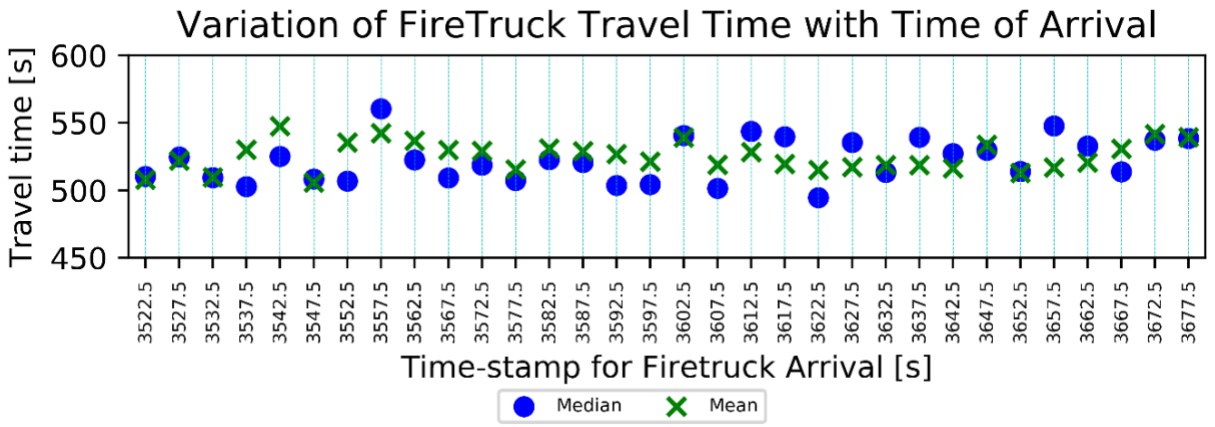

Figure 12 Variation of Travel Time for Fire Trucks depending on the time of arrival of the vehicle into the network

11.2 Dynamic Preemption vs Check-In Check-Out

As shown in

Figure 10 (b), the firetruck used in this experiment enters the network at the Southern part of the network and travels NB through 8 intersections, from the Medlock Bridge Road intersection to the Howell Ferry Road intersection, where it takes a right turn and leaves the corridor. Before further studying the effects of preemption, it is important to briefly discuss the merits of using the developed “dynamic preemption” (DP) algorithm as compared to a traditional “check-in check-out” (CI-CO) preemption strategy. For a CI-CO setup, a check-in detector is placed at a fixed distance from the intersection. When the EV reaches the detector, a preemption call is placed. The call remains active until the vehicle crosses a check-out detector (or times out), which is generally placed downstream

of the intersection. The drawback of this setup is experienced when an EV enters the back of a queue that extends past the check-in detector. In this situation the EV does not reach the check-in detector to trigger the preemption call. Using the DP approach to determine when to place the call while the EV is much further upstream avoids this issue as well as allows time to flush any queue ahead of the EV.

The trajectory plots in **Error! Reference source not found.** provide a visualization of the difference between these methods. The color in the EV trajectory represents the GREEN/AMBER/RED signal state of the next downstream intersection at the corresponding time. The blue line running in parallel to the trajectory represents the time-span of an active preemption call by the firetruck while traveling along its trajectory. **Error! Reference source not found.** (**a)** depicts one such scenario, with no preempt. It can be seen that the firetruck enters queues at various intersections (the vehicle stopping is represented by a flat line in the trajectory). **Figure 13 (b)** is for the same firetruck entry time, with preemption enabled with *normal* exit and a CI-CO implementation, where the detector is placed on an approach 1000 ft upstream of the intersection or immediately after the upstream intersection, whichever is less. **Figure 13 (c)** depicts the firetruck trajectory using DP to place preemption calls. The drawback of CI-CO is evident at the very first intersection. The firetruck is not able to place the call sufficiently early to allow for the queue to clear, instead being delayed in the queue while the downstream vehicles clear. The DP approach is able to clear the queue prior to the firetruck arrival, resulting in a significant reduction in delay. This same behavior reoccurs several times throughout the firetruck's trip. Over all, for the given arrival time and random seed in this example, CI-CO provides an 85s advantage over no-preempt while DP provides a 113s advantage,

providing a strong demonstration of the advantages of an approach, such as DP, leveraging CV data.

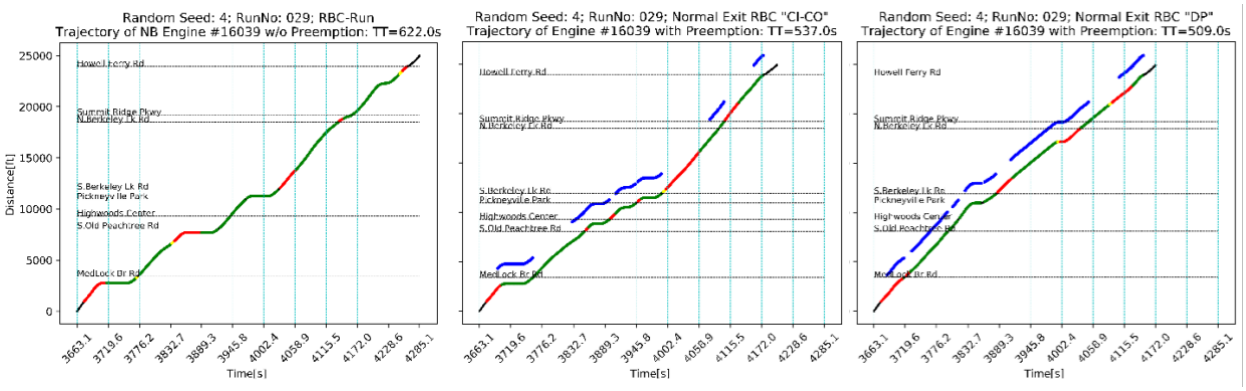

(a) **(b)** **(c)**

Figure 13 Difference in Firetruck Trajectory in the PIB VISSIM® network: (a) preemption disabled, (b) preemption enabled with *normal* exit - CI-CO, (c) preemption enabled with *normal* exit - DP

11.3 Corridor Analysis

Within this study the effects of preemption are studied via its impact on the travel times. The best EVP strategy would be one that would minimize EV delay, while also minimizing the negative effects on the other traffic, especially on the cross-streets (*12*). While the negative impacts of EVP are likely to be more pronounced on the side streets, it is possible that negative impacts may also be experienced by vehicles on the preemption approach. Therefore, this effort considers both the preemption approach and the cross-streets. To avoid the confounding effects of turn-related delays due to mixing of through and turn movement, the measurements in this study are made for vehicles involved only in through movements for both the main-line and cross-streets.

To study the impact of preemption on travel time, the results are aggregated over the 32 EV arrival times distributed over the cycle at the initial intersection, with five

replications of each, and are considered for three preemption strategies: no-preemption, *normal* exit transition, and *in-step* exit transition. First, **Error! Reference source not found. (a)** shows the travel time for non-EVs (i.e., general traffic) traveling the same route as the EVs. The travel time is reported from the initiation of the preemption call to the end of the call, then in 160 s intervals, allowing for visualization of the dissipation of any effect over multiple cycles. A vehicle's travel time is reported in this analysis when the vehicle started its trip. **Error! Reference source not found. (b)** shows the route travel time for the EVs. **Figure 15 (a) & (b)** are travel times for two representative cross streets, again aggregated over the 32 arrival times with 5 replicate trials, for the three preemption strategies.

Error! Reference source not found. & **Figure 15** utilize hybrid boxplots. The red square dots represent the mean, and the top and bottom of the solid box represent the 75th percentile and 25th percentile, respectively. The black line drawn on the solid box is the median; the whiskers around the box span within 1.5*IQR of the median and the points that lie beyond the whiskers are outliers (*36*). As seen in **Error! Reference source not found. (a)**, both the *normal* and *in-step* preemption strategies show significant improvement in travel time for the non-EVs. As the signals return more quickly to coordination when utilizing *in-step* exit transition, it is also seen that the non-EVs have the best performance when this transition strategy is utilized, particularly in the cycles immediately after the preemption call is placed. However, the positive effects of preemption is diminished as time passes and the gap between no-preemption (green boxes) and the preemption-enabled scenarios (yellow and blue boxes) is reduced progressively with the passage of each cycle. **Error! Reference source not found. (b)**

summarizes the travel time variation for the EV in the network under different preemption scenarios. The average travel time for no-preemption, preemption enabled with *normal* exit, and preemption-enabled with *in-step* exit, are 666 s, 526 s and 506 s, respectively with 140 s average travel time saved by preemption with *normal* exit compared to no-preemption. Furthermore, there is an additional improvement in travel time of 20 s when *in-step* exit is used as opposed to *normal* exit. Another positive aspect of preemption was a reduction in the variation of travel time as reflected by the reduced IQR, seen in both exit transition strategies. With the primary focus being on reducing EV delays, the choice of the strategy should be dictated by the optimal strategy for the EV. In this case, it was found that the *in-step* exit resulted in a small improvement over the *normal* exit, which is likely an effect of reduced interactions with other vehicles from the traffic stream, rather than a direct correlation with the signal timing. Hence *in-step* represents the superior strategy, within the constraints of the field conditions replicated in this study.

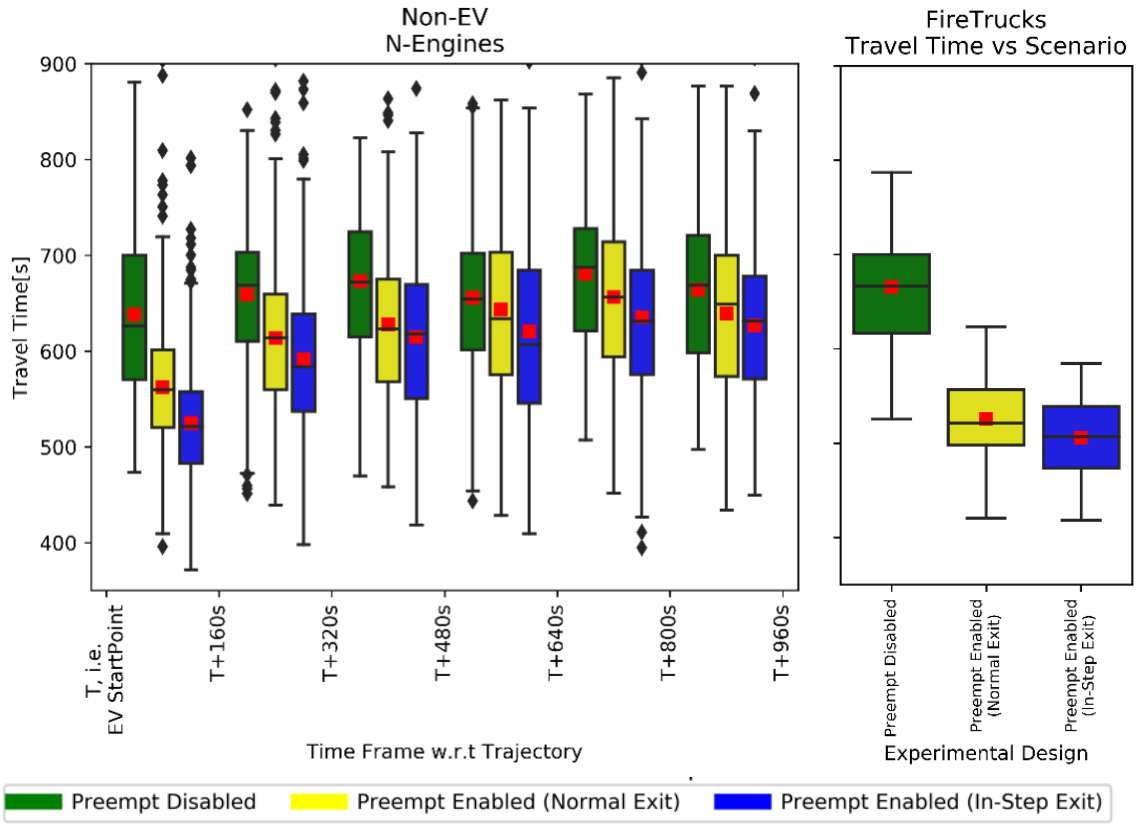

(a) **(b)**

Figure 14 Boxplots depicting variations in time taken to travel the entire NB Firetruck trajectory: (a) Non-EVs travelling since the arrival of the Firetruck, (b) Firetrucks.

Figure 15 (a) & (b) show how the travel time on the side streets is impacted by the three preemption strategies. As expected, the travel time increases immediately after the placement of the preemption call with the impacts rapidly dissipating. In addition, there is no clear trend between the *in-step* exit and *normal* Exit. This lack of one strategy clearly providing improved side street service was seen throughout the corridor side streets.

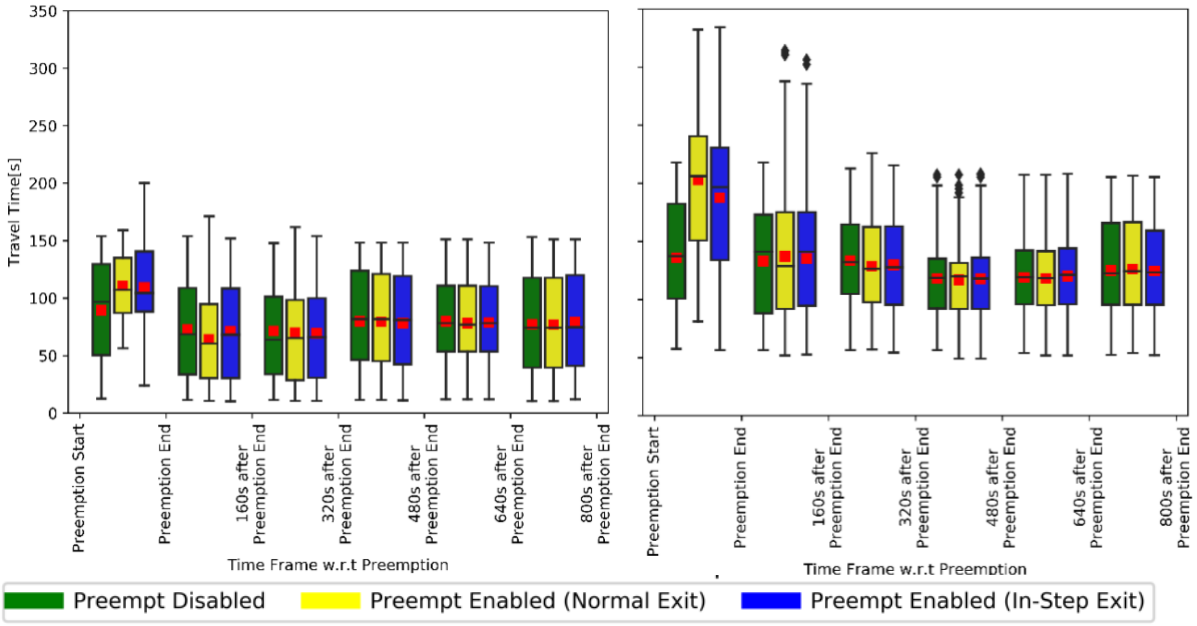

(a) **(b)**

Figure 15 Travel time comparison with varying preemption-design: Through movements for the side-streets during preemption and progressively after preemption: (a) WB-Through movement at PIB @South Berkeley Lake Road, (b) EB-through movement at PIB @North Berkeley Lake Road

12. CONCLUSION AND FUTURE WORK

This study demonstrates the positive effects of EVP combined with CV technology by implementing a DP architecture in a microscopic simulation model, using travel time as the primary metric. Preemption with *in-step* exit transition led to a 24% (160 s) reduction in average travel time for the firetruck. The non-EVs sharing the same path as the firetruck also received significant reduction in delay as a by-product of the preemption. When considering the side-street, it was observed there is a disruption in travel behavior on the side streets, leading to increased travel time with preemption. However, that effect on average travel time dissipated quickly. Also, neither the *in-step* or *normal* exit transitions proved to provide consistently superior service to the side streets. Therefore, considering

the effects on all traffic as a whole, preemption with *in-step* exit is a more favorable exit strategy for the network and conditions studied. However, generalization of these results will require additional study of other corridors and under varying traffic conditions.

Several improvements could be made on the experiment design that could provide for a more robust study. First, rather than choosing a mainline EV route, the route could be a mix of the main and side-streets. Second, scenarios with arrival of multiple EVs at an intersection should be explored to understand the interaction of overlapping preemption request calls. This could open doors to new possibilities of studying varying cases of delays in EV travel caused by preemption on the opposing movements. Third, there have been several studies tackling path planning problems for EVP (*19-21*). Since it was known the firetruck will only be traveling on the mainline utilizing a designated route, this is not included in the current experimental architecture. However, a probabilistic approach could be taken where the next intersection for a vehicle is predicted based on historical pathways and preemption call could be placed accordingly. Fourth, currently efforts are also being made to extend this study to use Software in the Loop Simulation (SILS) using *Intelight's MaxView® Advanced Traffic Management System* (ATMS) software (*37*). Lastly, while successful, the DP algorithm developed is a fairly simple heuristic. Additional refinement of the algorithm is merited. For instance, it was seen that the time of the preempt call relative to the local cycle can make a significant difference in performance. This may potentially be considered in setting when to place the call.

Beyond the EVP experimental design and algorithms a further enhancement to the model, to better represent the behavior in the field, would involve modeling of the potential pull-over behavior of non-EVs, whereby the vehicles move over to the shoulder or the

adjacent lane to create a clear path for the EV to bypass a queue. While the objective of the preemption is to avoid the need for such behavior, there are certainly conditions under which the congested conditions on the roadway might prevent the flushing of the queues at all intersections and pull-over behavior of the non-EVs may be necessary. A simulation environment modeling this behavior will allow for the study of strategies in gridlocked congestion situations. Additionally, for situations where the intersection is close to a fire station, there may not be sufficient time to clear the intersection. Consideration may need to be given to taking the intersection into an all-red state and allow the EV to go into the opposing lanes to cross the intersection. A modeling effort for such contraflow situations would allow for an evaluation of such strategies in addition to the strategies discussed in this paper.

While there are limitations to the work presented here, this effort provides and critically evaluates a novel idea of early detection of EV, as well as explores the effect of different preemption exit strategies, which could be a baseline architecture for informed real-time decision making integrating CV technology into the preemption strategy.

13. ACKNOWLEDGMENTS

The information, data, or work presented here was funded in part by the Gwinnett Department of Transportation and the Center for Transportation Equity Decisions & Dollars (CTEDD), a UTC funded by the USDOT. The authors thank Gwinnett DOT and CTEDD for support of this research. The authors would like to thank Mr. Tom Sever, Mr.

Alex Hoefflich, and Mr. Ken Keena from Gwinnett DOT for their unwavering support throughout the project.

14. AUTHOR CONTRIBUTIONS

The authors confirm contribution to the paper as follows: study conception and design: AG, MH, and SR; data collection: AG and SR; analysis and interpretation of results: MH, AG and SR; draft manuscript preparation: SR, AG, and MH. All authors reviewed the results and approved the final version of the manuscript.

References (Part I)

Bakula, C., Schneider, W. H., and Roth, J. (2012). "Probabilistic Model Based on the Effective Range and Vehicle Speed to Determine Bluetooth MAC Address Matches from Roadside Traffic Monitoring." Journal of Transportation Engineering, 138(1), 43-49.

Banks, J. H. (2009). "Automated analysis of cumulative flow and speed curves." Transportation research record, 2124(1), 28-35.

Barcelo, J., Montero, L., Marques, L., and Carmona, C. (2010). "Travel time forecasting and dynamic origin-destination estimation for freeways based on bluetooth traffic monitoring." Transportation Research Record(2175), 19-27.

Bertini, R. L. "Toward the systematic diagnosis of freeway bottleneck activation." Proc., Proceedings of the 2003 IEEE International Conference on Intelligent Transportation Systems, IEEE, 442-447.

Bertini, R. L., Lasky, M., and Monsere, C. M. "Validating predicted rural corridor travel times from an automated license plate recognition system: Oregon's frontier project." Proc., Intelligent Transportation Systems, 2005. Proceedings. 2005 IEEE, 296-301.

Brennan, T. M., Ernst, J. M., Day, C. M., Bullock, D. M., Krogmeier, J. V., and Martchouk, M. (2010). "Influence of vertical sensor placement on data collection efficiency from bluetooth MAC address collection devices." Journal of Transportation Engineering, 136(12), 1104-1109.

Charbonnier, S., Pitton, A.-C., and Vassilev, A. "Vehicle re-identification with a single magnetic sensor." Proc., 2012 IEEE International Instrumentation and Measurement Technology Conference, I2MTC 2012, May 13, 2012 - May 16, 2012, IEEE Computer Society, 380-385.

Chen, C., Skabardonis, A., and Varaiya, P. (2004). "Systematic identification of freeway bottlenecks." Transportation Research Record, 1867(1), 46-52.

Deng, M., Huang, J., Zhang, Y., Liu, H., Tang, L., Tang, J., and Yang, X. (2018). "Generating urban road intersection models from low-frequency GPS trajectory data." International Journal of Geographical Information Science, 32(12), 2337-2361.

Gong, L., and Fan, W. (2018). "Developing a systematic method for identifying and ranking freeway bottlenecks using vehicle probe data." Journal of transportation engineering, Part A: Systems, 144(3), 04017083.

Haghani, A., Hamedi, M., Sadabadi, K. F., Young, S., and Tarnoff, P. (2010). "Data collection of freeway travel time ground truth with Bluetooth sensors." Transportation Research Record(2160), 60-68.

Hainen, A. M., Wasson, J. S., Hubbard, S. M. L., Remias, S. M., Farnsworth, G. D., and Bullock, D. M. (2011). "Estimating route choice and travel time reliability with field observations of bluetooth probe vehicles." Transportation Research Record(2256), 43-50.

Hall, F. L., and Agyemang-Duah, K. (1991). "Freeway capacity drop and the definition of capacity." Transportation research record(1320).

Hofleitner, A., Herring, R., and Bayen, A. (2012). "Arterial travel time forecast with streaming data: A hybrid approach of flow modeling and machine learning." Transportation Research Part B: Methodological, 46(9), 1097-1122.

Kavaler, R., Kwong, K., Raman, A., Varaiya, P., and Xing, D. "Arterial performance measurement system with wireless magnetic sensors." Proc., 1st International Conference on Transportation Information and Safety: Multimodal Approach to Sustained Transportation System Development - Information, Technology, Implementation, ICTIS 2011, June 30, 2011 - July 2, 2011, American Society of Civil Engineers (ASCE), 377-385.

Kuroiwa, H., Kawahara, T., Kamijo, S., and Sakauchi, M. "Vehicle matching between adjacent intersections by vehicle type classification." Proc., 2006 IEEE International Conference on Systems, Man and Cybernetics, October 8, 2006 - October 11, 2006, Institute of Electrical and Electronics Engineers Inc., 389-394.

Kwong, K., Kavaler, R., Rajagopal, R., and Varaiya, P. (2009). "Arterial travel time estimation based on vehicle re-identification using wireless magnetic sensors." Transportation Research Part C: Emerging Technologies, 17(6), 586-606.

Lawson, T. W., Lovell, D. J., and Daganzo, C. F. (1997). "Using input-output diagram to determine spatial and temporal extents of a queue upstream of a bottleneck." Transportation Research Record, 1572(1), 140-147.

Li, P., and Souleyrette, R. R. (2016). "A generic approach to estimate freeway traffic time using vehicle ID-matching technologies." Computer-Aided Civil and Infrastructure Engineering, 31(5), 351-365.

Li, Y., and Li, Q. (2010). "A fast algorithm for identifying candidate links for floating car map-matching: a vector to raster map conversion approach." Annals of GIS, 16(3), 177-184.

Namaki Araghi, B., Krishnan, R., and Lahrmann, H. (2016). "Mode-specific travel time estimation using bluetooth technology." Journal of Intelligent Transportation Systems, 20(3), 219-228.

Newell, G. F. (1993). "A simplified theory of kinematic waves in highway traffic, part I: General theory." Transportation Research Part B: Methodological, 27(4), 281-287.

Qiu, Z., Cheng, P., Jin, J., and Ran, B. (2009). "Cellular probe technology applied in advanced traveller information system." World Review of Intermodal Transportation Research, 2(2), 247-260.

Quayle, S. M., Koonce, P., Depencier, D., and Bullock, D. M. (2010). "Arterial performance measures with media access control readers: Portland, Oregon, pilot study." Transportation Research Record(2192), 185-193.

Richardson, J. K., Smith, B. L., Fontaine, M. D., and Turner, S. M. (2011). "Network stratification method by travel time variation." Transportation Research Record(2256), 1-9.

Sanchez, R. O., Flores, C., Horowitz, R., Rajagopal, R., and Varaiya, P. "Arterial travel time estimation based on vehicle re-identification using magnetic sensors: Performance analysis." Proc., 14th IEEE International Intelligent Transportation Systems Conference, ITSC 2011, October 5, 2011 - October 7, 2011, Institute of Electrical and Electronics Engineers Inc., 997-1002.

Sanchez, R. O., Flores, C., Horowitz, R., Rajagopal, R., and Varaiya, P. "Vehicle re-identification using wireless magnetic sensors: Algorithm revision, modifications and performance analysis." Proc., Vehicular Electronics and Safety (ICVES), 2011 IEEE International Conference on, 226-231.

Turner, S., Albert, L., Gajewski, B., and Eisele, W. (2000). "Archived Intelligent Transportation System Data Quality: Preliminary Analyses of San Antonio TransGuide Data." Transportation Research Record: Journal of the Transportation Research Board, 1719(-1), 77-84.

Waddell, J. M., Remias, S. M., and Kirsch, J. N. (2020). "Characterizing Traffic-Signal Performance and Corridor Reliability Using Crowd-Sourced Probe Vehicle Trajectories." Journal of Transportation Engineering, Part A: Systems, 146(7), 04020053.

Waddell, J. M., Remias, S. M., Kirsch, J. N., and Trepanier, T. (2020). "Utilizing Low-Ping Frequency Vehicle Trajectory Data to Characterize Delay at Traffic Signals." Journal of Transportation Engineering, Part A: Systems, 146(8), 04020069.

Wagner, F. R. (2014). "PERSPECTIVES FROM THE FIELD: The Federal Highway Administration's "Every Day Counts" Initiative: Finding a Path to Better Environmental Outcomes within Existing NEPA and Agency Regulations." Environmental Practice, 16(4), 347-348.

Xu, C., Liu, P., Yang, B., and Wang, W. (2016). "Real-time estimation of secondary crash likelihood on freeways using high-resolution loop detector data." Transportation research part C: emerging technologies, 71, 406-418.

Xu, T. D., Sun, L. J., Peng, Z. R., and Hao, Y. "Modelling drivers' en-route diversion behaviour under variable message sign messages using real detected traffic data." Institution of Engineering and Technology, 294-301.

Zhang, L., and Levinson, D. (2004). "Some properties of flows at freeway bottlenecks." Transportation Research Record, 1883(1), 122-131.

Zhao, W., McCormack, E., Dailey, D. J., and Scharnhorst, E. (2013). "Using truck probe GPS data to identify and rank roadway bottlenecks." Journal of Transportation Engineering, 139(1), 1-7.

REFERENCES (Part II)

[1] Office, I. T. S. J. P. Connected Vehicle Pilot Deployment Program. USDOT. https://www.its.dot.gov/pilots/ Accessed July 30, 2021.

[2] Knox, J. The Region's Connected Vehicle Technology is Getting Ready to Roll. Atlanta Regional Commision (ARC). https://atlantaregional.org/whats-next-atl/articles/the-regions-connected-vehicle-technology-is-getting-ready-to-roll/. Accessed July 30, 2021.

[3] Kwon, E., S. Kim, and R. Betts. Route-based dynamic preemption of traffic signals for emergency vehicle operations.In Transportation Research Board 82nd Annual MeetingTransportation Research Board, 2003.

[4] Hong, K.-S., J.-H. Jung, and G.-H. Ahn. Development of the Emergency Vehicle Preemption Control System Based on UTIS. The Journal of The Korea Institute of Intelligent Transport Systems, Vol. 11, No. 2, 2012, pp. 39-47.

[5] Wang, Y., Z. Wu, X. Yang, and L. Huang. Design and implementation of an emergency vehicle signal preemption system based on cooperative vehicle-infrastructure technology. Advances in Mechanical Engineering, Vol. 5, 2013, p. 834976.

[6] Eliminator. Preemption System - Emergency Vehicle - Transit. Collison Control Communications. https://collisioncontrol.net/PreemptionSystems/?gclid=Cj0KCQiApt_xBRDxARIsAAMUMu_IjJEiTe4k0tnTcFLBTB6GNLLJ1F9WstFXn0ty2tgO5SPZwVc1syoaAqMyEALw_wcB. Accessed July 27, 2021.

[7] Technologies, G. T. Central Management Software (CMS) for Traffic Signal Priority Control. Global Traffic Technologies. www.gtt.com/project/central-management-software-cms-for-traffic-signal-priority-control/. Accessed July 27, 2021.

[8] Emtrac. EMTRAC Systems Signal Priority: Emergency Vehicle Preemption (EVP) Utilizing ITS Functionality. https://www.emtracsystems.com/first-response/emergency-vehicle-preemption-evp/. Accessed July 27, 2021.

[9] Information, A. Emergency Vehicle Preemption and Priority System: Applied Information. appinfoinc.com/solutions/preemption-priority/. Accessed July 27, 2021.

[10] Manual on Uniform Traffic Devices for Streets and Highways (MUTCD), 2009 Edition. United States Department of Transportation, Federal Highway Administration, Washington D.C. https://mutcd.fhwa.dot.gov/pdfs/2009/pdf_index.htm. Accessed August 1, 2021.

[11] Traffic Signal Timing Manual: Chapter 9. United States Department of Transportation, Federal Highway Administration, Washington D.C. https://ops.fhwa.dot.gov/publications/fhwahop08024/chapter9.htm#9.1. Accessed July 23, 2021.

[12] Shaaban, K., M. A. Khan, R. Hamila, and M. Ghanim. A strategy for emergency vehicle preemption and route selection. Arabian Journal for Science and Engineering, Vol. 44, No. 10, 2019, pp. 8905-8913.

[13] WSDOT, T. Traffic signal priority & preemption. WSDOT. https://tsmowa.org/category/signal-operations/traffic-signal-priority-preemption. Accessed July 29, 2021.

[14] Nelson, E. J., and D. Bullock. Impact of emergency vehicle preemption on signalized corridor operation: An evaluation. Transportation research record, Vol. 1727, No. 1, 2000, pp. 1-11.

[15] Ten, H., Y. Qi, J. C. Falcocchio, K.-B. Kim, R. Patel, and E. Athanailos. Simulation testing of adaptive control, bus priority and emergency vehicle preemption in New York City.In Transportation Research Board 82nd Annual MeetingTransportation Research Board, 2003.

[16] McHale, G. M., and J. Collura. Improving emergency vehicle traffic signal priority system assessment methodologies.In Transportation Research Board 82nd Annual MeetingTransportation Research Board, 2003.

[17] Yun, I., B. B. Park, C. K. Lee, and Y. T. Oh. Comparison of emergency vehicle preemption methods using a hardware-in-the-loop simulation. KSCE Journal of Civil Engineering, Vol. 16, No. 6, 2012, pp. 1057-1063.

[18] Homaei, H., S. Hejazi, and S. A. M. Dehghan. A new traffic light controller using fuzzy logic for a full single junction involving emergency vehicle preemption. Journal of Uncertain Systems, Vol. 9, No. 1, 2015, pp. 49-61.

[19] Gedawy, H. K., M. Dias, and K. Harras. Dynamic path planning and traffic light coordination for emergency vehicle routing. Comp. Sci. Dept., Carnegie Mellon Univ., Pittsburgh, Pennsylvania, USA, Vol. 189, 2008.

[20] Saravanan, R., P. V. Paul, M. Nivedha, and B. Nirosha. Optimal path planning and traffic signal control system for emergency vehicle—A survey.In 2017 International Conference on Computation of Power, Energy Information and Commuincation (ICCPEIC), IEEE, 2017. pp. 283-289.

[21] Zhao, J., Y. Guo, and X. Duan. Dynamic path planning of emergency vehicles based on travel time prediction. Journal of advanced transportation, Vol. 2017, 2017.

[22] PTV, A. PTV VISSIM® 2021 user manual. PTV AG: Karlsruhe, Germany, 2021.

[23] Python. Python 3.7.0 Release. https://www.python.org/downloads/release/python-370/. Accessed June 25, 2020.

[24] OpenStreetMap. OpenStreetMap. https://www.openstreetmap.org/. Accessed Aug. 1, 2021.

[25] Google. Google Maps: Peachtree Industrial Boulevard. https://www.google.com/maps/dir/33.9459033,-84.2363882/34.0064816,-84.1701493/@33.9949555,-84.2917807,11679m/data=!3m1!1e3!4m2!4m1!3e0. Accessed July 27, 2021.

[26] Trucano, T. G., L. P. Swiler, T. Igusa, W. L. Oberkampf, and M. Pilch. Calibration, validation, and sensitivity analysis: What's what. Reliability Engineering & System Safety, Vol. 91, No. 10-11, 2006, pp. 1331-1357.

[27] Wiedemann, R. Simulation des Strassenverkehrsflusses. 1974.

[28] Anderson, J., W. Suh, A. Guin, M. Hunter, and M. O. Rodgers. Accounting for composite travel time distributions within a traffic stream in determining Level-of-Service. Journal of Intelligent & Fuzzy Systems, Vol. 36, No. 2, 2019, pp. 955-965.

[29] Dowling, R., A. Skabardonis, and V. Alexiadis. Traffic analysis toolbox, volume III: Guidelines for applying traffic microsimulation modeling software.In, United States. Federal Highway Administration. Office of Operations, 2004.

[30] (RITIS), R. I. T. I. S. Regional Integrated Transportation Information System (RITIS). https://www.ritis.org/traffic/. Accessed July 28, 2021.

[31] PTV, A. PTV VISSIM®- 3D Vehicle Models. PTV AG: Karlsruhe, Germany. https://company.ptvgroup.com/en-us/ptv-vissim-3d-vehicle-models. Accessed July 28, 2021.

[32] Tiaprasert, K., Y. Zhang, X. B. Wang, and X. Zeng. Queue length estimation using connected vehicle technology for adaptive signal control. IEEE Transactions on Intelligent Transportation Systems, Vol. 16, No. 4, 2015, pp. 2129-2140.

[33] Li, J.-Q., K. Zhou, S. E. Shladover, and A. Skabardonis. Estimating queue length under connected vehicle technology: Using probe vehicle, loop detector, and fused data. Transportation research record, Vol. 2356, No. 1, 2013, pp. 17-22.

[34] PTV, A. PTV VISSIM® 2021: RBC user manual. PTV AG: Karlsruhe, Germany, 2014.

[35] Taylor, C. Understanding the Interquartile Range in Statistics. ThoughtCo. https://www.thoughtco.com/what-is-the-interquartile-range-3126245. Accessed August 1, 2021.

[36] Galarnyk, M. Understanding Boxplots. towards data science. https://towardsdatascience.com/understanding-boxplots-5e2df7bcbd51. Accessed July 30, 2021.

[37] Intelight. MaxView: Advanced Traffic Management System. https://amsignalinc.com/data-sheets/Intelight/Intelight-MaxView-Product-Sheet.pdf. Accessed July 27, 2021.

Appendix B: Technology Transfer

An Appendix should be included in this final report to document the Technology Transfer activities conducted during the project term, accomplishments towards T2 adoption and implementation by relevant stakeholders, as well as any relevant post-project T2 plans.

CENTER FOR TRANSPORTATION EQUITY, DECISIONS & DOLLARS

The **Center for Transportation, Equity, Decisions and Dollars (CTEDD)** is a USDOT University Transportation Center, leading **transportation policy research** that aids in **decision making** and **improves economic development** through **more efficient, and cost-effective use of existing transportation systems,** and offers **better access to jobs and opportunities.** We are leading a larger consortium of universities focused on **providing outreach** and **research to policy makers**, through **innovative methods** and **educating future leaders of the transportation field.**

UNIVERSITY OF TEXAS ARLINGTON

CAL POLY SAN LUIS OBISPO

Georgia Tech

USF UNIVERSITY OF SOUTH FLORIDA

WISCONSIN UNIVERSITY OF WISCONSIN–MADISON

C-TEDD@UTA.EDU CTEDD.UTA.EDU @UTACTEDD @ C__TEDD @ CENTER FOR TRANSPORTATION, EQUITY, DECISIONS AND DOLLARS 817.272.5138